PREMIO TESI DI DOTTORATO

– 35 –

PREMIO TESI DI DOTTORATO

Commissione giudicatrice, anno 2012

Luigi Lotti, *Facoltà di Scienze Politiche* (Presidente della Commissione)

Fortunato Tito Arecchi, *Facoltà di Scienze Matematiche, Fisiche e Naturali*
Franco Cambi, *Facoltà di Scienze della Formazione*
Paolo Felli, *Facoltà di Architettura*
Michele Arcangelo Feo, *Facoltà di Lettere e Filosofia*
Roberto Genesio, *Facoltà di Ingegneria*
Mario Pio Marzocchi, *Facoltà di Facoltà di Farmacia*
Adolfo Pazzagli, *Facoltà di Medicina e Chirurgia*
Mario Giuseppe Rossi, *Facoltà di Lettere e Filosofia*
Salvatore Ruggieri, *Facoltà di Medicina e Chirurgia*
Saulo Sirigatti, *Facoltà di Psicologia*
Piero Tani, *Facoltà di Economia*
Fiorenzo Cesare Ugolini, *Facoltà di Agraria*
Vincenzo Varano, *Facoltà di Giurisprudenza*
Graziella Vescovini, *Facoltà di Scienze della Formazione*

Roberta Gualdani

Using the Patch-Clamp technique to shed light on ion Channels Structure, Function and Pharmacology

Firenze University Press
2013

Using the Patch-Clamp technique to shed light on ion channels structure, function and pharmacology / Roberta Gualdani. – Firenze : Firenze University Press, 2013.
(Premio FUP. Tesi di dottorato ; 35)

http://digital.casalini.it/9788866554530

ISBN 978-88-6655-452-3 (print)
ISBN 978-88-6655-453-0 (online)

Peer Review Process
All publications are submitted to an external refereeing process under the responsibility of the FUP Editorial Board and the Scientific Committees of the individual series. The works published in the FUP catalogue are evaluated and approved by the Editorial Board of the publishing house. For a more detailed description of the refereeing process we refer to the official documents published in the online catalogue of the FUP (http://www.fupress.com).

Università degli Studi di Firenze
Firenze University Press
Borgo Albizi, 28, 50122 Firenze, Italy
http://www.fupress.com/
Printed in Italy

Contents

Roberta Gualdani, *Using the Patch-Clamp technique to shed light on ion channels structure, function and pharmacology*, ISBN 978-88-6655-452-3 (print), ISBN 978-88-6655-453-0 (online)

Abstract

Ion channels are membrane proteins that allow the selective conduction of ions across the cellular membrane down their electrochemical gradient; they regulate a variety of functions such as neuronal excitability, heartbeat, muscle contraction and hormones release.

During my PhD thesis, by combining electrophysiology with site-direct mutagenesis, fluorophore labelling experiments and pharmacological assays, I explored the structural rearrangements in the cardiac Na^+/Ca^{2+} exchanger (Chapter II); the role of some amino acids on Ca^{2+} sensitivity of human BK_{Ca} channel (Chapter III); the pharmacological effects of natural and chemical drugs on hERG K^+ channel (ChapterIV) and TRPA1 (Chapter V) channel.

The first project investigated the structural rearrangements of the cardiac Na^+/Ca^{2+} exchanger (NCX) during its operation using the Cut-Open Oocyte Voltage-Clamp Fluorometry technique (COVF).

NCX is a plasma membrane protein that exchanges three Na^+ for one Ca^{2+}; it is found in many tissues but it is particularly abundant in the heart where, by extruding Ca^{2+} after each contraction, NCX controls heart contractility. To understand the mechanisms of Na^+ and Ca^{2+} translocation in NCX we have expressed the cardiac NCX in *Xenopus laevis* oocytes and site-directed fluorescent labelling of extracellularly exposed cysteines serving as binding sites for fluorophores with sulfhydryl reactive groups was achieved. The emission of these fluorescent probes is sensitive to the surrounding environment reporting a structural change in their proximity. COVF allowed us to monitor ionic currents and structural rearrangements of protein. Our results indicate that it is possible to detect NCX current by cut-open oocyte voltage-clamp technique with a high signal/noise ratio. The wild-type NCX, possessing four extracellular endogenous cysteines (Cys14, Cys20, Cys122 and Cys792), was incubated prior to voltage clamp with the thiol-reactive fluorescent dye tetramethyl rhodamine-5-maleimide (TMRM) which reported changes in fluorescence emission correlating with changes in NCX activity, as induced by changing the external $[Ca^{2+}]$. Our results suggest that one or more cysteines, close to the $\alpha 1$ and $\alpha 2$ regions, experience a change in the surrounding environment during NCX activation.

The aim of the second project was to understand the role of αG - βG loop of RCK1 domain on BK channels Ca^{2+} sensitivity.

Large Conductance Ca^{2+}- and Voltage-dependent K^+ channels (BK_{Ca}) play key roles in regulating vascular tone, action potential duration and firing, hormone se-

Roberta Gualdani, *Using the Patch-Clamp technique to shed light on ion channels structure, function and pharmacology*, ISBN 978-88-6655-452-3 (print), ISBN 978-88-6655-453-0 (online)

cretion and muscle relaxation. Elevation of intracellular [Ca^{2+}] in the micromolar range dramatically increases the apparent voltage sensitivity of the channel. However, the molecular mechanism underlying Ca^{2+}-dependent regulation of the BK_{Ca} channels is unknown. Strong evidence suggests that two RCK (Regulators of K^+ Conductance) domains constitute a large part of the BK_{Ca} channel C-terminus and are responsible for its Ca^{2+} sensitivity, nevertheless the structural organization and mode of operation of these modules remain unresolved.

The RCK1 domain contains three residues critical for high-affinity Ca^{2+} sensitivity: D362, D367 and M513. We have constructed a 3D homology model of RCK1 based on the structure of a bacterial RCK domain showing that D362/367 map within the N-lobe, while M513 is part of the αG-βG loop. Interestingly, two charged residues, R514 and K518 are in proximity of D362/367, adjacent to M513. Moreover, the αG-βG loop connecting the N and C lobes of RCK1 includes three consecutive negative residues: 520EED522. We have investigated the effect of charge neutralization/substitution at positions R514, K518 and EED520-2 on the Ca^{2+}-dependent activation of the human BK_{Ca} channel expressed in *Xenopus* oocytes using the patch clamp technique; our results show a relevant role of the αG-βG region of the BK_{Ca} RCK1 domain in channel activation.

The last project of this thesis explored the pharmacological effect of natural and chemical drugs on two different ion channels: the human-ether-a-go-go-related gene (hERG) K^+ channel and the Transient Receptor Potential Ankiryn 1 (TRPA1) channel.

hERG K^+ channel plays a critical role in the action potential; this protein is blocked by a number of compounds and its inhibition can lead to cardiac arrhythmia and long QT syndrome. As a consequence, preventing the proarrhythmic risk of hERG blockade is recognized as a major hurdle in the preclinical development of new drugs. To this purpose, by patch clamp measurements on hERG-expressing *Xenopus laevis* oocytes, we have investigated the hERG blocking potential of two novel antimalarial drugs; these data, in the context of intended preclinical and clinical studies, provides an important benchmark for cardiac risk assessment.

TRPA1 channel is expressed in sensory neurons and has increasingly emerged as relevant for nociception. This protein is activated by pungent compounds, such as the constituents of mustard oil (MO), cinnamon and garlic; moreover it mediates the inflammatory actions of environmental irritants (e.g. ROS, noxious cold temperature) and analgesic agents.

Parthenolide, traditionally used in Europe to treat inflammatory diseases, is a sesquiterpene lactone derived from the leaves of *Tanacetum parthenium*. Its biological activity is thought to be mediated through the α-methylene-γ-lactone moiety on its structure; however, the mechanism by which this occurs and the molecular target of Parthenolide are unclear.

To understand this question, by electrophysiological experiments, we demonstrated that Parthenolide activates TRPA1 channel in a concentration-dependent manner and elicits desensitization and cross-desensitization in CHO cells expressing

hTRPA1. Moreover, we showed that the triple mutant hTRPA1 (C619A C639A C663A) is less sensitive to Parthenolide, in compare to wild-type, similarly to other TRPA1 agonists.

Introduction

1.1 Ion Channels and life

Cellular life is defined by the compartmentalization of a set of reactions that transforms energy from the environment (heat, light, chemical bonds) into more readily usable forms. Cellular energy is stored in chemical bonds (e.g., ATP) and in potential gradients across membranes.

Gradients of ionic species are particularly powerful and the machinery of the cell responsible for ion trafficking are ion channels and transporters. These are integral membrane proteins that facilitate the passage of ions from one side of the membrane to the other. Transporters utilize cellular energy (chemical or gradient) to actively shuttle ions across the membrane, and are thus capable of establishing ion gradients. Ion channels, on the other hand, are passive devices and form transmembrane pores that allow the selective conduction of ions down their electrochemical gradient (Figure 1.1).

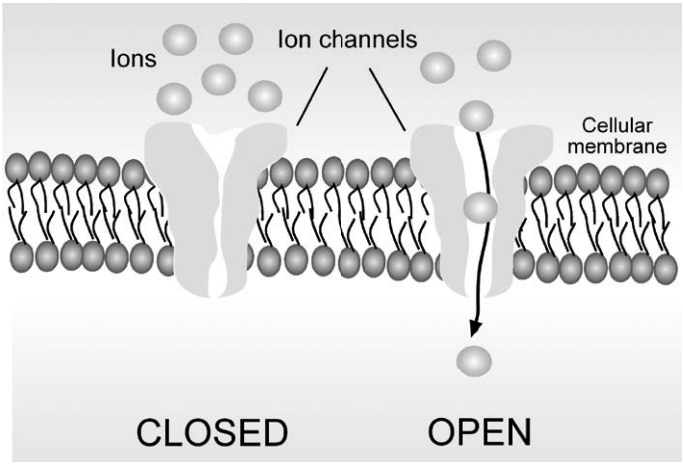

Figure 1.1 Schematic representation of an ion channel in the closed (left) and open (right) state. In the closed conformation ions are blocked by a gate, whereas opening of the gate allows ions to flow from one side of the cell to the other.

Roberta Gualdani, *Using the Patch-Clamp technique to shed light on ion channels structure, function and pharmacology*, ISBN 978-88-6655-452-3 (print), ISBN 978-88-6655-453-0 (online)

It is well established that ion channels play a vital role a variety of functions such as neuronal excitability, cardiac cycle, muscle contraction and hormones release (Hille 2001).

In particular ion channels play three principal physiological roles:

1. They set up the resting membrane potentials of the cells (e.g. for neurons typical values of the resting potential range from –70 to –80 mV). Since the flow of ions moves charge and constitutes an electric current, channel opening and closing determine all electrical signals of excitable cells such as nerve and muscle.
2. The flux of ions through ion channels contributes to the electrolyte movements required for volume regulation of single cells and for the transport of salt across epithelial tissues.
3. A few ions make regulatory signals inside cells. For example some cytoplasmic signals are generated by the opening of Ca^{2+} channels that let Ca^{2+} ions flow into the cytoplasm. The Ca^{2+} may come from the extracellular medium or from intracellular organelles. This Ca^{2+} release is the primary mechanism for translation of electrical signals into chemical signals.

Remarkably the existence of ion channels was only postulated and verified quite recently. It has been known since the middle of last century that large currents flowed across biological membranes. For example in 1952 A.L. Hodgkin and A.F Huxley (Nobel Prize in Physiology or Medicine, 1963) carried out a study of the ionic basis of nerve impulse and measured the conductance of sections of nerve in giant squid axon. The conductance measured in such experiments was quite large, in the order of $2x10^{-2}\ \Omega^{-1}cm^{-2}$, so they supposed the existence of a mechanism for transporting ions across the membrane. Furthermore, Hodgkin and Huxley deduced that this ion permeation occurred at localized sites in the membrane.

The development of the patch-clamp technique in 1976 (E. Neher and B. Sakmann, Nobel Prize in Physiology or Medicine, 1991) shed further light on the situation (see Paragraph 1.4). Indeed it was found that current flows through small isolated sections of membrane in identifiable *quanta*, supporting the idea of 'ion channels'. In fact, these experiments have measured, for the first time, the current passing through single channels (Sackmann and Neher 1995).

1.2 Ion Channels properties

Gating

Ion channel 'gating' means opening and closing of the ion conduction pore in response to a specific stimulus. Some channels open in response to specific ligand molecules binding (ligand-gated channels); others open in response to membrane voltage (voltage-gated channels) or to mechanical pressure (mechano-sensitive channels).

The exact process of channel gating is not well known and, in any case, varies between the different types of channels. Voltage-gated channels contain a section of the protein known as the 'voltage sensor', which is highly charged and moves in response to potential changes opening the channel (Bezanilla 2003). In ligand-gated ion channels, the energy gained in binding the ligand to the extracellular domain of the protein is used to produce channel activation (Purves et al. 2001).

Structure

Ion channels are composed of one or more pore-forming subunits, often in association with accessory subunits. Most channels conform to a common structural theme in which the central pore, through which the ions translocate, is formed by four or five transmembrane a-helices, which fit together like the staves of a barrel. In many channels, the pore-forming helices belong to separate subunits, so the channel is tetrameric (K_{ir} channels, for example) or pentameric (Cys-loop receptors). On the contrary, voltage-gated Ca^{2+} (Ca_V) and Na^+ (Na_V) channels are composed of a single subunit that contains four similar repeated domains, and some K^+ channels are dimers, each subunit being composed of two repeated domains (Ashcroft 2006).

Knowledge of the three-dimensional atomic structure of channels is important for understanding the mechanism underlying channel function; moreover knowing which atoms line the pore, or the location of charged groups is essential to make a detailed model of the interactions between the ions and the channel.

The conventional method for determining protein structure has been X-ray crystallography. In this technique, a channel of interest is crystallized and studied by shining X-rays from various angles and analyzing the diffraction pattern. Unfortunately, membrane proteins, and channels in particular, are difficult to crystallize and they are only stable in their native conformation when surrounded by the lipid membrane. However the similarities in amino acid sequences gives the possibility to deduce the approximate structure of a large number of channels, by using computational tools to model ion channels (Homology modeling, Electrostatics calculations, Molecular dynamics simulations) (Tai et al. 2008).

The breakthrough in determining biological ion channel structure was made in 1998 when, for the first time, the *KcsA* potassium channel from *Streptomyces lividans* structure was obtained using X-ray crystallography (Figure 1.2).

Although it is significantly simpler than most potassium channels in human cells, the *KcsA* channel has a very similar mechanism of function and is thought to contain an essentially similar pore forming structural core of other K^+ channels. Furthermore, Na^+ and Ca^{2+} channels are believed to have evolved from K^+ channels and share many characteristics in the pore-forming region of these channels (Lodish et al., 2000).

The *KcsA* channel is around 45 Å in length. The inner end of the pore appears to be an 18 Å long tunnel, around only 6 Å in diameter. The center of the channel contains a 10 Å diameter cavity. The outer end of the pore is believed to be responsible

for the channel ability to select which cation passes through it. Both end of the pore contain negatively charged regions which prevent anions from entering the channel.

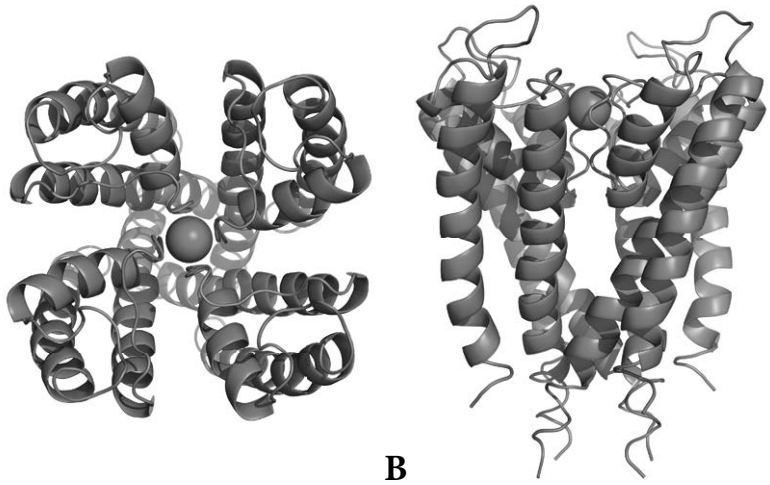

Figure 1.2 Crystal structure of KcsA (PdB code 1BL8 A). Stereoview of a ribbon representation illustrating the KcsA tetramer viewed from the extracellular side. B) Stereoview from another perspective, perpendicular to that in A) (Doyle et al. 1998).

Recently, many crystal structures have been obtained for a number of ion channels and the big technological advances in crystallography make us to think that more channel structure can be expected in the near future.

Selectivity

Ion channels, like enzymes, have their specific substrates: potassium, calcium, sodium and chloride channels permit only K^+, Ca^{2+}, Na^+ or Cl^- ions to diffuse through their central pores. Ion selectivity is the ability of an ion channel to discriminate among different ions.

First of all the discrimination between anions and cations is based on their charge; for example the K^+ selectivity filter contain carbonyl oxygen (negative charges), while the Cl^- selectivity filter contain amide nitrogen atoms (positive charges) (Roux et al. 2011).

Moreover discrimination between ions with the same charge appears to be more complex, rely for example on different size or on different hydration energy (Morais-Cabral et al. 2001).

1.3. Ion Channels as drug-target

The role of ion channels in drug preclinical development has emerged as an important issue in the last several years. Many drugs have been removed from the mar-

ket because they prolong the cardiac QT interval and, in several cases, produce a lethal ventricular arrhythmia known as *torsade de pointes* (Sanguinetti and Tristani-Firouzi 2006). The mechanism underlying this toxic effect involves the inhibition of one or more of the cardiac ion channels: i) the hERG K^+ channel (I_{kr}); ii) the KCNQ1/KCNE1 potassium channel (I_{ks}); iii) the SCN5A sodium channel.

Moreover mutations that disrupt or alter channel function have been associated with many diseases ('channelopathies'), including hypertension, cardiac arrhythmia, diabetes, cystic fibrosis, and a variety of neuronal disorders. Thus, ion channels represent an important class of molecular targets for drug development (Ashcroft 2006).

Channel-mediated ion flux is determined by the number of channels in the membrane, the fraction of time they remain open (the open probability) and the conductance of the single channel. Any alteration of these properties could disrupt channel function; for this reason understanding the detailed mechanisms of channel function will help discover how to combat these pathologies.

1.4. The Patch-Clamp technique

The standard technique for high-resolution recording of the ionic currents flowing through a cell membrane is known as 'patch-clamp' (Neher and Sakmann 1995).

The principle of this method is to electrically isolate a patch of membrane from the external solution and to record current flowing into the patch. This is achieved by pressing a glass micropipette (1-3 μm tip), which has been filled with an isotonic saline solution, against the surface of a cell and applying light suction (Figure 1.3). Under such conditions a seal, whose electrical resistance is more than 1 GΩ is formed; this reduces the current noise of the recording and allows a good resolution of single channel currents, whose amplitude is the order of pA.

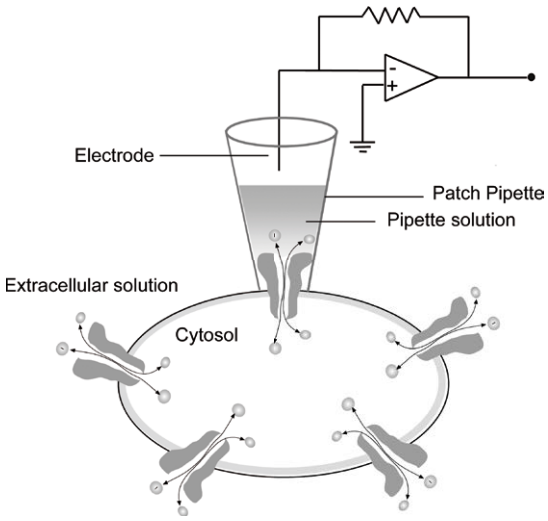

Figure 1.3 Schematic diagram of the patch-clamp setup.

There four different configurations for the patch technique: cell-attached patch, whole cell recording, and excised patch (outside-out patch and inside-out patch).

The cell-attached patch configuration is used to measure the currents of single ion channels of the intact cell.

The whole-cell recording is achieved when additional negative pressure is applied to the cell membrane as it is in the cell-attached configuration. The suction through the pipette causes the rupture of the cell membrane; in this case, the solution of the pipette enters into the cytoplasm and the current passing through the entire cell membrane is recorded.

In the inside-out configuration, after the seal formation, the micropipette is quickly detached from the cell, thus breaking a patch of membrane that remains attached to the micropipette, and exposing the intracellular side of the membrane to the external solution. This is useful when it's necessary to manipulate the environment at the cytoplasmic surface of an ion channel. For example, channels that are activated by intracellular ligands can be studied through a range of different ligand at different concentrations.

In the outside-out configuration, after the whole-cell patch is formed, the electrode is pulled far away, the patch of membrane detaches from the cell and turns into a convex membrane, with the original outside of the membrane facing outward from the electrode. Outside-out patching gives the experimenter the opportunity to examine the properties of an ion channel when it is isolated from the cell, and exposed to different analytes on the extracellular side.

1.5. The Cut-Open Voltage-Clamp Fluorometry technique (COVCF)

The *Xenopus laevis* oocyte is the most common heterologous expression system of transporters and ion channels (Goldin 2006).

To measure currents, two different electrophysiological techniques are currently used: (a) the two microelectrode voltage clamp for recording whole-oocyte currents; (b) the patch clamp for studying single channel currents.

However, these techniques have some technical drawbacks:

- two electrode voltage clamp doesn't allow fast solution exchange and resolution of currents with fast kinetics;
- in two electrode voltage clamp the internal medium is not accessible and this limitation reduces the range of possible experiments and can cause a contamination of the recorded currents by endogenous components of oocytes, such as the calcium-activated chloride channels;
- for patch clamp studies, the average survival time of the patch is generally < 1 h.

The Cut-Open Voltage Clamp technique (COVG) overcomes the limitations of both methods (Stefani and Bezanilla 1998, Gandhi and Olcese 2008).

In this procedure, the oocyte is inserted in a chamber that separates the surface into three regions. The top portion of the oocyte membrane is the region that is

clamped at a reference potential (holding potential) and is the section from which currents are recorded. The middle portion is a 'guard' that is clamped to the same potential as the top. The bottom portion is the region of the oocyte that is 'cut-open', by permeabilization with saponin, a detergent like protein that solubilizes cholesterol leaving much of the membrane structure intact; in this way it is possible to modify the chemical composition of the internal environment and to inject current inside the cell, through a low resistance pathway.

Other important advantages of this method are: low noise recording of ion channels current and stable recording conditions for several hours.

The Voltage-Clamp Fluorometry (VCF) combines the Cut-Open Voltage Clamp technique with a scanning cysteine accessibility mutagenesis (SCAM). In this method a channel of interest is modified by engineered cysteines introduced at specific positions and expressed in *Xenopus laevis* oocytes (Mannuzzu et al. 1996). The cysteines are then selectively modified with an organic thiol-reactive fluorophore probe (two commonly used fluorophores are PyMPO maleimide and TMRM tetramethylrhodamine maleimide).

Structural rearrangements during channel gating are assayed via fluorescence emission differences caused by changes in the local environment around the fluorophore (e.g. a change in membrane potential or a change from aqueous to lipid phase). Such an environmental change is reported as a negative/positive DF as a consequence of an increase/decrease in residue solvent-accessible surface area.

The examination of the DF (dimming or brightening) derived from different residues shows that each amino acid has unique fluorescence emission, even in adjacent positions. This indicates that the fluorophore senses a small region of space in the vicinity of the residues to which it is attached, and that moving the attachment in an adjacent position means pointing in a different direction where there are different interactions with the surrounding environment (Figure 1.4). In other words, VCF provides information about protein motion in real-time and at a single amino acid resolution.

The fluorescence is monitored at a fixed wavelength with a photomultiplier tube, CCD camera, or photodiode while the ionic current is controlled with a voltage-clamp apparatus.

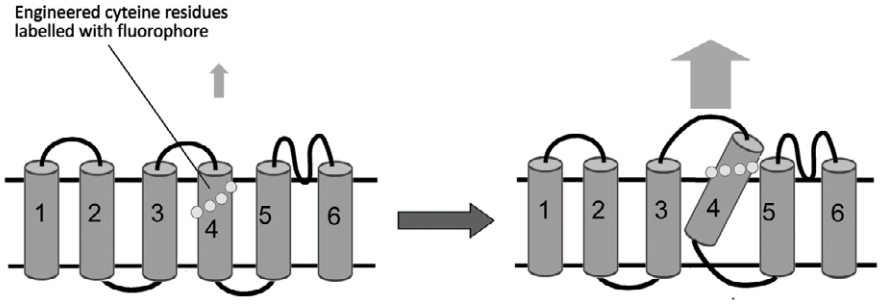

Figure 1.4 Engeneered cyteine residues of an ion channel are selectively selectively modified by an organic thiol-reactive fluorophore probe; a conformational rearrangement alters the

fluorescent tag's surrounding environment and this change is reported as a ΔF as a consequence of an increase or decrease in residue solvent-accessible surface area.

References

Ashcroft F.M. (2006) From molecule to malady. *Nature* 440, 440-447.

Bezanilla F. (2003) The Voltage Sensor in Voltage-Dependent Ion Channels. *Physiol. Rev.* 80, 555-592.

Doyle D.A., Cabral J.M., Pfuetzner R.A., Kuo A., Gulbis J.M., Cohen S.L., Chait B.T., MacKinnon R. (1998) The Structure of the Potassium Channel: Molecular Basis of K^+ Conduction and Selectivity. *Science* 280, 69-77.

Dutzler R., Campbell E.B., Cadene M., Chait B.T., MacKinnon R. (2002) X-ray structure of a ClC chloride channel at 3.0 Å reveals the molecular basis of anion selectivity. *Science* 415, 287-294.

Gandhi C.S. and Olcese R. (2008) The Voltage-Clamp Fluorometry Technique. *Methods in Molecular Biology, Potassium Channel* 491, Chapter 17.

Goldin, A. L. (2006) Expression of Ion Channels in Xenopus Oocytes, in Expression and Analysis of Recombinant Ion Channels: From Structural Studies to Pharmacological Screening. Weinheim, FRG: Wiley-VCH Verlag GmbH & Co. KGaA.

Hille B. (2001) *Ionic Channels of Excitable Membranes.* Sunderland, MA: Sinauer Associates, Inc.

Hodgkin A., Huxley A. (1952) A quantitative description of membrane current and its application to conduction and excitation in nerve. *J. Physiol.* 117, 500–544.

Lodish H., Berk A., Zipursky S.L., Matsudaira P., Baltimore D., Darnell J. (2000) *Molecular Cell Biology*. New York: W.H. Freeman.

Mannuzzu L.M., Moronne M.M., Isacoff. E.Y. (1996) Direct physical measure of conformational rearrangement underlying potassium channel gating. *Science* 271, 213–216.

Morais-Cabral J.H., Zhou Y., MacKinnon R. (2001) Energetic optimization of ion conduction rate by the K^+ selectivity filter. *Nature* 414, 37-42.

Purves D., Augustine G.J., Fitzpatrick D., Katz L.C., LaMantia A-S., McNamara J.O. (2001) *Neuroscience*. Sunderland (MA): Sinauer Associates.

Roux B., Bernèche S., Egwolf B., Lev B., Noskov S.Y., Rowley C.N., Yu H. (2011) Ion selectivity in channels and transporters. *J. Gen. Physiol.* 137, 415-426.

Sackmann B., Neher E. (1995) *Single-Channel Recording.* New York: Plenum Press.

Sanguinetti M.C., Tristani-Firouzi M. (2006) hERG potassium channels and cardiac arrhythmia. *Nature* 440, 463–469.

Stefani E. and Bezanilla F. (1998) Cut-Open Oocyte Voltage-Clamp Technique. *Methods in Enzymology* 293, 300-318.

Tai K., Fowler P., Mokrab Y., Stansfeld P., Sansom S.P. (2008) Molecular Modeling and Simulation Studies of Ion Channels Structures, Dynamics and Mechanisms. *Methods In Cell. Biology* 90, 233-265.

Ye S., Li Y., Chen L., Jiang Y. (2006) Crystal Structures of a Ligand-free MthK Gating Ring: Insights into the Ligand Gating Mechanism of K^+ Channels. *Cell* 126, 1161-73.

Structural rearrangements of cardiac Na^+/Ca^{2+} Exchanger (NCX1) revealed by Cut-Open Voltage Clamp Fluorometry

2.1 Function and Topology of NCX1: State of the Art

Ca^{2+} is utilized by cells as a ubiquitous signalling molecule, and changes in its concentration control a number of physiological pathways (second messengers and neurotransmitters release, muscle contraction and relaxation, fertilization). Alteration in the function or regulation of any of these events has serious and deleterious consequences, often associated with the pathogenesis of disease.

Among the different proteins that mediate Ca^{2+} movement, Na^+/ Ca^{2+} exchanger (NCX) is the predominant mechanism for Ca^{2+} efflux across the cell (Philipson and Nicoll 2000, Lytton 2007).

However, under pathological conditions, regulatory mechanisms are overwhelmed and intracellular calcium concentration ($[Ca^{2+}]_i$) increases through calcium influx from extracellular pools via various channels and, under extreme circumstances, via the Na^+/Ca^{2+} exchanger (NCX). These conditions can cause cell death.

The most recent topology of NCX contains 9 transmembrane segments (TMSs) in the N-terminus and 4 TMSs in the C-terminus, separated by a large cytosolic loop (Figure 2.1). The large intracellular loop contains regulatory sites including Na^{+}-dependent exchange inhibitor peptide (XIP), Ca^{2+} binding sites and two alternatively spliced regions (Ottolia et al. 2009, John et al. 2011).

Accessibility experiments indicate that the $\alpha 1$ and $\alpha 2$ regions are oriented in opposite directions with respect to the membrane and their central regions form membrane re-entrant loops that have limited accessibility to both sides of the membrane (Iwamoto et al. 2000, Nicoll et al. 1999). Furthermore cross linking experiments have localized the helices predicted to flank the α-repeats in each other proximity (Ren et al. 2006).

Moreover the $\alpha 1$ and $\alpha 2$ regions are highly conserved amino acids sequences and mutagenesis experiments suggest that they significantly contribute to ion binding and translocation (Ottolia et al. 2005).

Roberta Gualdani, *Using the Patch-Clamp technique to shed light on ion channels structure, function and pharmacology*,
ISBN 978-88-6655-452-3 (print), ISBN 978-88-6655-453-0 (online)

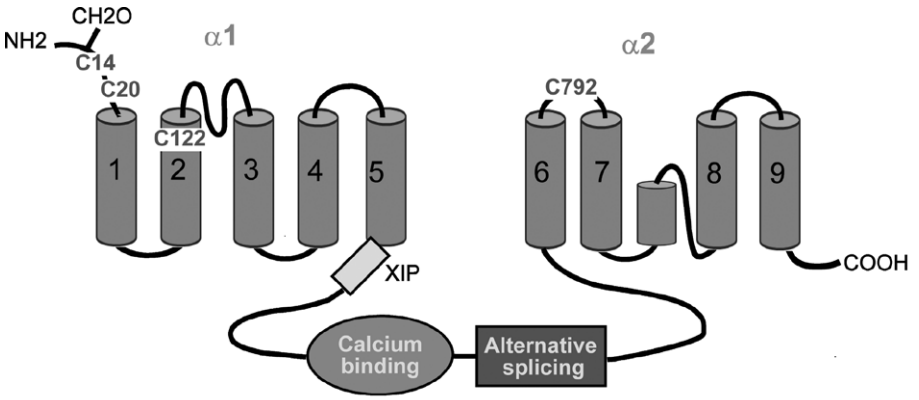

Figure 2.1 Topological model of NCX1. Adapted from (Philipson and Nicoll 2000).

Operation of the Na^+/Ca^{2+} exchanger is fully reversible and the direction of ion movement depends on the electrochemical gradient of Na^+ (Figure 2.2). For NCX1, the stoichiometry of ion transport has been investigated and a value of three Na^+ ions in exchange for one Ca^{2+} ion has generally been accepted; this means that NCX1 transport is electrogenic, and thus can be measured using electrophysiological techniques.

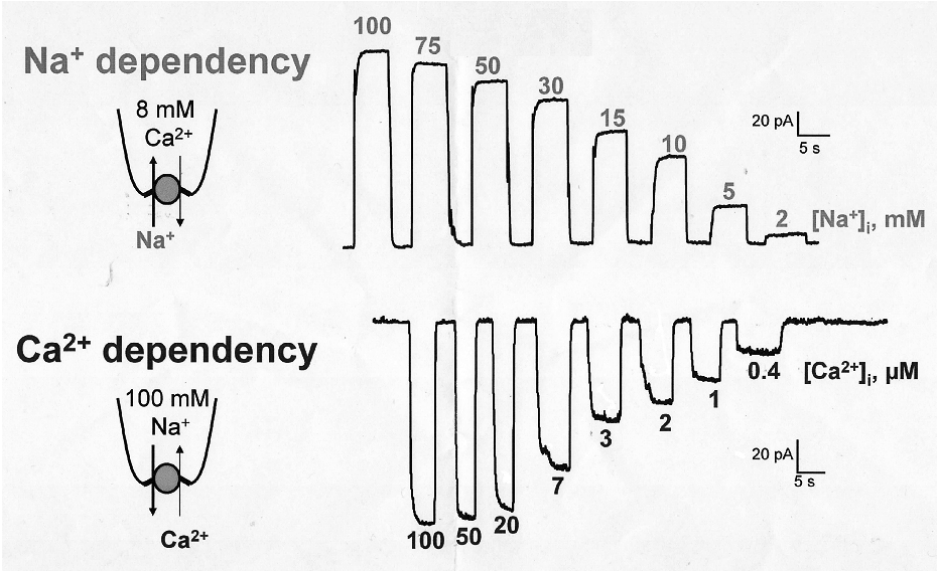

Figure 2.2 Representative outward (top) and inward currents (bottom) recorded from an oocyte membrane patches expressing NCX1. Outward exchange currents (top) were measured in the presence of the 8 mM Ca^{2+} in the pipette and varying cytoplasmic Na^+, while inward currents (bottom) were obtained with 100 mM Na^+ in the pipette and varying intracellular Ca^{2+}. Adapted from (Ottolia et al. 2005).

The cytosolic region of Na^+/Ca^{2+} exchanger is particularly important because the binding of Na^+ and Ca^{2+} ions to the large intracellular loop of the protein activates or inhibits ion current. Figure 2.3 shows the secondary Na^+ and Ca^{2+} regulation of the cardiac Na^+-Ca^{2+} exchanger, measured by giant patch technique in *Xenopus laevis* oocytes. Ca^{2+} ions are constantly present within the pipette, and outward exchange currents are elicited by applying Na^+ into the bath at the intracellular surface. Regulatory Ca^{2+} is also present as shown.

The left panel demonstrates Na^+-dependent inactivation: upon application of internal Na^+, outward exchange current peaks and then inactivates to a new steady-state level.

The right panel demonstrates Ca^{2+} regulation; in this case, the level of regulatory Ca^{2+} in the bath was 15 μM instead of 1 μM. Two properties are evident. First, the Na^+-dependent inactivation is eliminated in the presence of high regulatory Ca^{2+}, so Ca^{2+} modulates Na^+ regulation. Second, upon removal of regulatory Ca^{2+}, transporter activity declines to zero; this means that Ca^{2+} is transported by the exchanger but also exerts a separate regulatory effect.

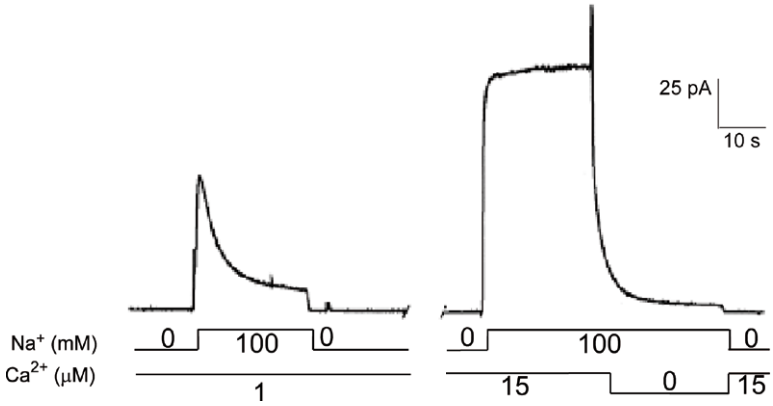

Figure 2.3 Typical current traces demonstrating cytoplasmic Ca^{2+} and Na^+ regulation of outward Na^+/Ca^{2+}exchange (NCX) currents obtained from inside-out giant patch oocyte. Currents were induced by the rapid application of 100 μM Na^+ to the cytoplasmic side of the patch at the indicated intracellular Ca^{2+} concentrations. Adapted from (Philipson and Nicoll 2000).

2.2 Fluorometric measurements of conformational changes in NCX1

Relatively little is known about the conformational changes that accompany ion-coupled transport of NCX. It is thought that NCX mediates Na^+/Ca^{2+} exchange through a reaction cycle with conformational changes between two access states that alternatively expose the ion binding sites to the extracellular or to the intracellular solution (Figure 2.4). However, there is no direct evidence for the conformational changes that occur during the transport cycle.

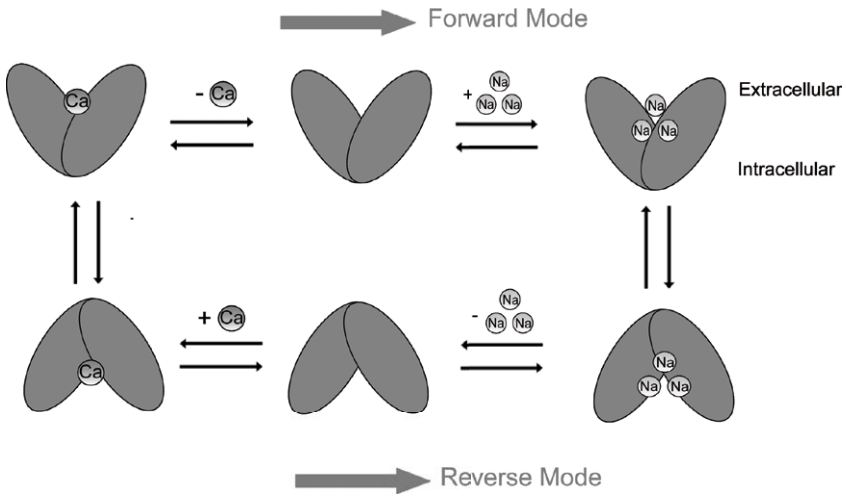

Figure 2.4 The NCX1 cycle (reverse and forward mode). Operation of Na^+/Ca^{2+} exchanger is reversible and the direction of ion movement depends on the electrochemical gradient of Na^+. Adapted from (Lytton 2000)

Recent crystallographic studies of secondary transporters have greatly advanced our understanding of transporter function; however, this mechanistic description is derived from a patchwork of different transporters crystallized in different states (Dang et al. 2010). For this reason an accurate and complete description of the exact conformational changes that a given transporter undergoes during ion transport doesn't exist.

In this project we are investigating the conformational changes of NCX by using the Cut-Open oocytes Voltage-Clamp Fluorometry (VCF) technique (see Chapter 1). This technique was originally used to study conformational changes in potassium channels during the gating process (Pantazis et al. 2010, Savalli et al. 2006). More recently, VCF was also used to investigate glucose transporter (Meinild et al. 2002), glutamate transporter (Larsson et al. 2004), serotonin transporter (Li and Lester 2002), and Na^+-K^+ pump (Geibel et al. 2003).

Based on this technique, cysteine residues -endogenous or introduced by site-direct mutagenesis- of a protein (ion channel or transporter) are selectively labelled with a thiol-reactive fluorophore probe (e.g. tetramethyl rhodamine-5-maleimide TMRM) and the protein is expressed in *Xenopus laevis* oocytes.

The cut-open oocyte technique (COVG) is very suitable for ionic current recording of NCX because this protein elicits small current that requires high expression level and low noise recording. Moreover fluorescence recordings allow to detect structural movement of the protein because the fluorophore is sensitive to its local environment and any environmental change that causes an increase/decrease in residue solvent-accessible surface area is reported as a negative/positive ΔF.

The Na^+-Ca^{2+} exchanger contains internal regions of sequence homology known as the alpha repeats ($\alpha 1$ and $\alpha 2$ regions), which are thought to be involved in ion

translocation and transport. Furthermore NCX possesses only four extracellular endogenous cysteines (Cys14, Cys20, Cys122 and Cys792), located in proximity of α1 and α2 regions, that could serve as binding sites for fluorophores with sulfhydryl reactive groups (e.g. tetramethyl rhodamine-5-maleimide, TMRM). For this reason we concentrated our investigation in proximity of α1 and α2 regions, to explore ionic currents and ΔF related to extracellular cysteines movement during NCX operation.

2.3 Methods

Oocyte Preparation, cRNA Injection, Fluorescent Labelling

Oocytes were dissected from anesthetized *Xenopus leavis* (African clawed frogs) by surgical harvest of oocytes. Oocytes were immediately treated with collagenase (2mg/mL) for 1.5 hours, rinsed with a Ca^{2+}-free OR-2 solution (82.5 mM NaCl, 2.5 mM KCI, 1 mM $MgCl_2$, 5 mM Hepes-NaOH pH 7.6) and stored in SOS solution (96 mM NaCl, 2 mM KCI, 1.8 mM $CaCl_2$, 1 mM $MgCl_2$, 5 mM Hepes-NaOH pH 7.6) containing fresh penicillin (100 units/ ml), streptomycin (100 μg/ml), gentamycin (50 μg/ml).

In vitro RNA transcription was performed with the "mMessage mMachine" kit (Ambion) with T7 RNA polymerase.

Oocytes were injected with 50 nl of cRNA and maintained at 18°C in an amphibian saline solution supplemented with 50 mg/ml gentamycin/200 μM DTT (to prevent the oxidation of free sulfhydryl residues of endogenous cysteines in the protein) /10 μM EDTA (a metal chelator) for 2-7 days before experiments. Before starting fluorescence recordings, oocytes were incubated 30-40 min. at room temperature in a labelling solutions containing 10 μM SH-reactive fluorescent dye TMRM (tetramethyl rhodamine-5-maleimide).

COVG Fluorometry

Fluorescence and ionic currents were recorded in voltage clamp condition by using the COVG implemented for fluorescence measurements.

Fluorescence and ionic currents were acquired from a membrane area of ~ 0.28 mm^2, isolated by the recording chamber, and amplified by an Amplifier CA-1 (DAGAN Corp., Minneapolis, MN). The lower part of the oocyte in contact with the internal solution was permeabilized with saponin 0.1% to lower the access resistance to the oocyte interior. The optical setup included a Zeiss AXIOSCOPE FS-PLUS with a ACROPLAN 40x objective (Carl Zeiss, Iena, Germany). Excitation filters, dichroic mirrors, and emission filters were appropriate for tetramethyl rhodamine-5-maleimide (Gandhi 2008)

Solutions used for COVG Fluorometry: external solution was 120 mM CsMES, 2 mM $Mg(MES)_2$ or $Ca(MES)_2$, 10 mM Hepes, 0.1 mM ouabaine and 0.2 mM flufenamic acid (two blockers of endogenous Cl^- current in oocytes); internal solu-

tion was 120 mM NaMES, 10 mM Hepes, 10 mM BAPTA (a chelator of cytoplasmic Ca^{2+} to remove endogenous Ca^{2+}-dependent Cl^- current in oocytes); micropipette solution was 3 M KMES, 10 mM HEPES; picospritzer solution was 80 mM $Ca(MES)_2$, 10 mM HEPES.

Outward currents and ΔF were triggered by replacement of Mg^{2+} (NCX non-substrate) with Ca^{2+} (NCX substrate) solutions, in presence of intracellular Na^+. For all solutions, pH = 7.0. COVG recordings were performed at 30°C, VCF recordings at room temperature.

'Giant' patch measurements

Outward NCX currents were recorded using the giant patch technique (Hilgemann 1995). Borosilicate glass pipettes were pulled and fire-polished to a final inner diameter of about 20–30 μm and coated with a mixture of Parafilm and mineral oil. Prior to experiments, the vitelline membrane of the oocyte was removed manually in an isotonic solution identical to the solution for seal formation. After membrane excision, solutions were rapidly changed using a computer-controlled 20-channel solution switcher.

Na^+ and Ca^{2+} activation curves were obtained by perfusing solutions with different ion concentrations. Experiments were performed at 35 °C and at a holding potential of 0 mV.

2.4 Results

Na^+-dependency of NCX labelled with the fluorophore TMRM

First we examined if the TMRM fluorophore labelling could modify the physiological mechanism of NCX.

To this purpose, by giant-patch technique, we determine the apparent affinities for Na^+ of NCX, by measuring outward exchange currents generated by application of different cytoplasmic Na^+ concentrations with 8 μM extracellular Ca^{2+} within the pipette. Moreover, because application of Na^+ at the extracellular surface induces a slow inactivation process, the exchanger was 'deregulated' by treatment with chymotrypsin at the intracellular surface (Hilgemann 1995).

As we can observe in Figure 2.5, the Na^+-affinity curves of NCX labelled (green) and not-labelled (yellow) with TMRM are very similar; this means that TMRM doesn't significantly alter Na^+-transport mediated by NCX.

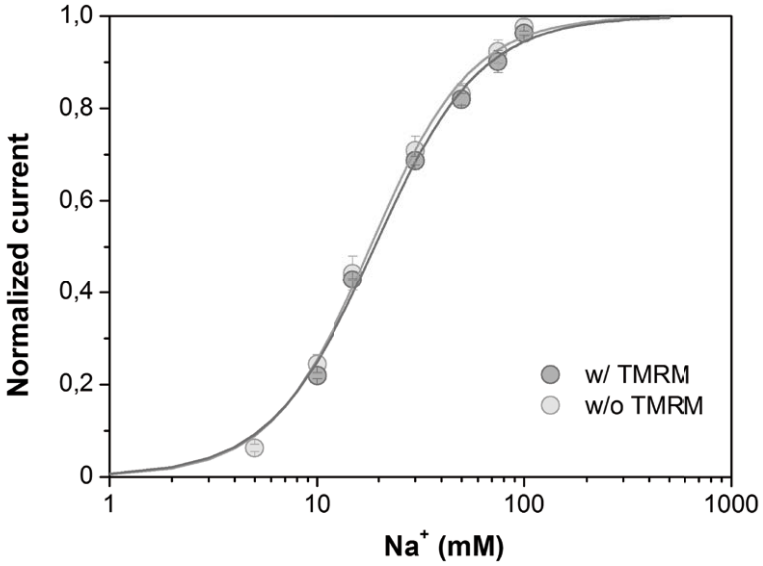

Figure 2.5 Na^+-dependency from oocytes expressing wild type NCX labelled (dark grey) and not-labelled (light grey) with TMRM.

Outward NCX currents of wild-type and K229Q+Δ680-5 mutant

We decided to concentrate our attention on K229Q+DΔ680-5 NCX mutant, because it lacks $[Ca^{2+}]_i$-dependent regulation and $[Na^+]_i$-dependent inactivation of wild-type NCX; for this reason its activity is higher and easier to modulate compare to wild-type.

In Figure 2.6 are shown representative NCX currents obtained from an excised oocyte membrane giant patch expressing NCX wild-type (top) and K229Q+DΔ680-5 mutant (bottom). Currents were activated by replacing 100 mM Cs^+ with 100 mM Na^+ on the cytoplasmic surface of the patch. Currents were activated also in the presence or absence of regulatory Ca^{2+} (5 μM) on the cytoplasmic surface.

K229Q+DΔ680-5 mutant, contrary to what was observed in wild-type, is not inactivated by Na^+, as seen by the lack of a current transient when Na^+ is applied to the bath. Moreover is also not modulated by Ca^{2+}; in fact, removal of Ca^{2+} from the bathing solution does not affect exchanger currents.

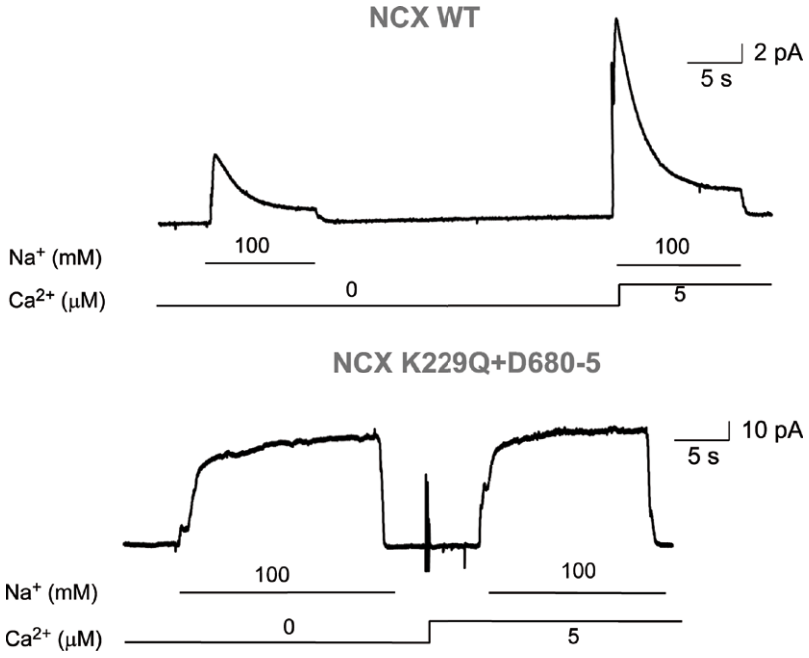

Figure 2.6 Representative outward NCX currents obtained from an excised oocyte membrane patch expressing wild-type Na^+/Ca^{2+} exchanger (top) and K229Q+DΔ680-5 mutant (bottom).

Cut-Open Oocyte Voltage Clamp (COVC) recording of Na^+/Ca^{2+} exchanger

To study NCX activity, we employed, for the first time, the Cut-Open Oocyte Voltage Clamp recording technique. This technique allows reproducible manipulation of the internal and external ionic environment of the oocyte: this is very important for NCX recordings, because NCX current amplitude depends on the electrochemical gradient of Na^+ and COVC allows to increase cytoplasmic Na^+, by adding NaMES to the intracellular compartment of oocyte.

In Figure 2.7 is shown a COVC recording from an oocyte expressing an exchanger mutant lacking cytoplasmic Na^+-dependent inactivation and which does not required cytosolic Ca^{2+} for activation (mutant K229Q+Δ680-5).

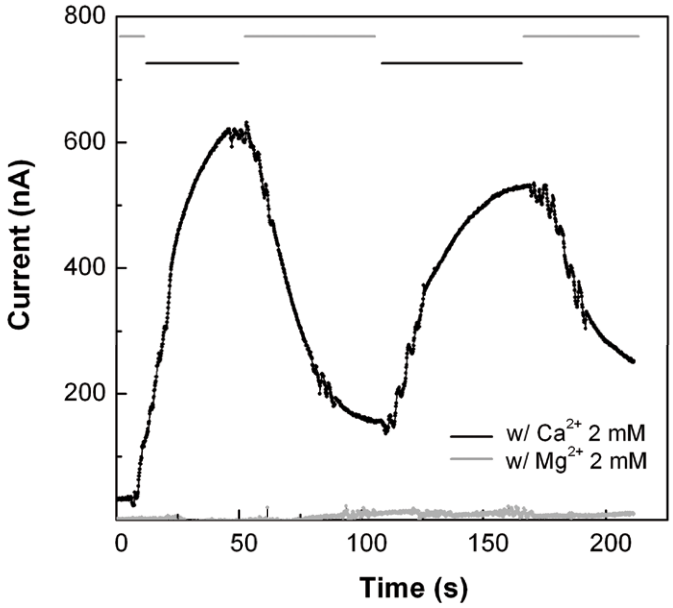

Figure 2.7 Cut-Open Oocyte Voltage Clamp recordings (holding potential + 40 mV) from an oocyte uninjected (grey) and expressing (black) K229Q+Δ680-5 NCX mutant.

Outward current was triggered by application of 2 mM Mg^{2+} (NCX non-substrate) or 2 mM Ca^{2+} (NCX substrate) solutions, in presence of intracellular Na^{+}. Only in presence of Ca^{2+} NCX elicits big and reversible currents (black), following the electrochemical gradient of Na^{+}, that is more concentrated in the cytoplasmic site of the oocyte. The signal is over-imposed with the current generated by an uninjected oocyte, in the same ionic condition (green).

This big ionic current can be ascribed to NCX because:

- it resembles the shape of the current recorded from an excised oocyte membrane giant patch expressing NCX (Figure 2.6 bottom);
- the signal is reversible because it follows the exchange of solution between Mg^{2+} and Ca^{2+};
- it's activated only when both Na^{+} and Ca^{2+} are present on the opposite sides of the cellular membrane;
- it's recorded only from oocytes expressing NCX.

Voltage-Clamp Fluorometry (VCF) recording of Na^{+}/Ca^{2+} exchanger

In Figure 2.8 is shown a VCF recording of Na^{+}/Ca^{2+} exchanger labelled with TMRM. Each arrow indicates a 'puff' (a volume of solution ≤ 1 μl, ejected on top of the oocyte) of 80 mM Ca^{2+} solution.

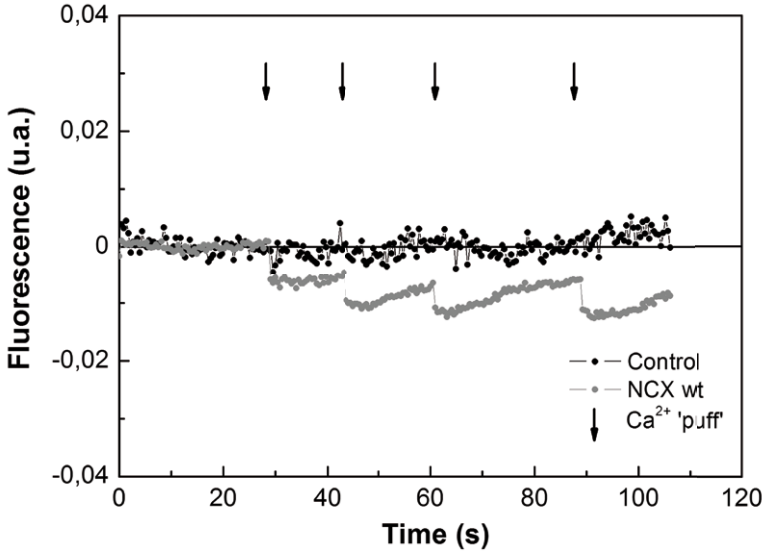

Figure 2.8 Example of VCF recording from an oocyte uninjected (black) and expressing Na^+/Ca^{2+} exchanger (grey), both labelled with TMRM; each black arrow indicates a 'puff' of 80 mM Ca^{2+} solution.

In Figure 2.8, the oocyte expressing NCX shows a fast and reversible fluorescence quenching (red trace) when Ca^{2+} is added to the extracellular solution. Uninjected oocytes serve as the negative control (Figure 2.8, black trace).We concluded that changes in fluorescence emission, induced by changing the external solution (with or without Ca^{2+}), can be correlated with changes in NCX activity, suggesting that one or more endogenous extracellular cysteines (Cys14, Cys20, Cys122 and Cys792), located in proximity of α1 and α2 regions are experiencing a change in the surrounding environment during NCX activation.

2.5 Discussion

Our project focuses on the conformational dynamics and structural rearrangements of the cardiac Na^+/Ca^{2+} exchanger (NCX1) during its operation, using Cut-Open Voltage-Clamp Fluorometry.
Our preliminary results can be summarized as follows:

TMRM labelling doesn't alter the Na^+-transport mediated by NCX (Figure 2.6);

COVC is a promising technique for investigating NCX activity, allowing to record NCX current with a high signl/noise ratio (Figure 2.7).

VCF recordings from NCX labelled with TMRM shows a fast and reversible fluorescence quenching, when Ca^{2+} is added to the extracellular solution; this suggests that one or more NCX endogenous cysteines (between Cys14, Cys20, Cys122 and Cys792, the only exposed extracellularly) experience a change in the surrounding environment during transporter activation (Figure 2.8).

In summary our preliminary data support the idea that α1 and α2 regions are involved in the structural rearrangements of NCX during ion translocation and encourage us to rationally explore, by site-directed fluorescent labeling, all key residues of NCX, in the region close to the α1 and α2 motifs, with the aim to completely identify the amino acids involved in the conformational movements of the transporter during activation.

References

Dang S., Sun L., Huang Y., Lu F., Liu Y., Gong H., Wang J. and Yan N. (2010). Structure of a fucose transporter in an outward-open conformation. *Nature* 467, 734-739.

Gandhi C.S. and Olcese R. (2008) The Voltage-Clamp Fluorometry Technique. *Methods in Molecular Biology, Potassium Channel* 491, Chapter 17.

Geibel S., Kaplan J.H., Bamberg E. and Friedrich T. (2003) Conformational dynamics of the Na^+/K^+-ATPase probed by Voltage Clamp Fluorometry. *PNAS* 100, 964-969.

Hilgemann D.W. (1995) *The giant membrane patch. in Single Channel Recording,* New York: Plenum (eds. Sackmann B, Neher E.), 307–327.

Iwamoto T., Uehara A., Imanaga I. and Shigekawa M. (2000) The Na^+/Ca^{2+} exchanger NCX1 has oppositely oriented re-entrant loop domains that contain conserved aspartic acids whose mutation alters its apparent Ca^{2+} affinity. *J. Biol. Chem.* 275, 38571–38580.

John S.A., Ribalet B., Weiss J.N., Philipson K.D., Ottolia M. (2011) Ca^{2+}-dependent structural rearrangements within Na^+-Ca^{2+} exchanger dimers. *PNAS* 108, 1699-1704.

Larsson H.P., Tzingounis A.V., Koch H.P., Kavanaugh M.P. (2004) Fluorometric measurements of conformational changes in glutamate transporters. *PNAS* 101, 3951-3956.

Lytton J. (2007) Na^+/Ca^{2+} exchangers: three mammalian gene families control Ca^{2+} transport. *Biochem. J.* 406, 365-382.

Li M. and Lester H.A. (2002) Early Fluorescence Signals Detect Transitions at Mammalian Serotonin Transporters. *Biophys. J.* 83, 206-218.

Meinild A.K., Hirayama B.A., Wright E.M., and Loo D. (2002) Fluorescence Studies of Ligand-Induced Conformational Changes of the Na^+/Glucose Cotransporter. *Biochemistry* 41, 1250-1258.

Nicoll D.A., Ottolia M., Lu L., Lu Y. and Philipson K.D. (1999) A new topological model of the cardiac sarcolemmal Na^+-Ca^{2+} exchanger. *J. Biol. Chem.* 274, 910–917

Ottolia M., Nicoll D.A. and Philipson K.D. (2005) Mutational Analysis of the α-1 Repeat of the Cardiac Na^+-Ca^{2+} Exchanger. *J. Biol. Chem.* 280, 1061-1069.

Pantazis A., Gudzenko V., Savalli N., Sigg D., Olcese R. (2010) Operation of the voltage sensor of a human voltage and Ca^{2+}-activated K^+ channel. *PNAS* 107, 4459-4464.

Philipson K.D. and Nicoll D.A, (2000) Sodium-Calcium Exchange: A Molecular Perspective. *Annu. Rev. Physiol.* 62, 111-133.

Ren X., Nicoll D. A. and Philipson K. D. (2006) Helix packing of the cardiac Na^+-Ca^{2+} exchanger: proximity of transmembrane segments 1, 2, and 6. *J. Biol. Chem.* 281, 22808–22814.

Savalli N., Kondratiev A., Toro L., Olcese R. (2006) Voltage-dependent conformational changes in human Ca^{2+} and voltage-activated K^+ channel, revealed by voltage-clamp fluorometry. *PNAS* 103, 12619-12624.

Calcium Sensitivity in the human BK_{Ca} channel: the role of loop αG - βG in the RCK1 domain

3.1 BK_{Ca} channels and Physiology

Large-Conductance, Voltage- and Ca^{2+}-dependent K^+ channels (BK_{Ca}), are ubiquitous membrane proteins that play fundamental and well-established roles in controlling smooth muscle tone and neuronal excitability, as well as serving as oxygen and carbon monoxide sensors (Cui et al. 2009, Hou et al. 2008).

Biophysical properties of BK_{Ca} channels include their large conductance and dual sensitivity to both voltage and intracellular calcium ions (Horrigan and Aldrich 2002, Latorre and Brauchi 2006, Yuan et al. 2010). Moreover their K^+ conductance of ~250 pS is an order of magnitude larger than that observed in typical voltage-gated K^+ channels, making the BK channel a powerful regulator of the cell membrane potential.

An example of the physiological importance of BK_{Ca} channels is their localization in presynaptic nerve termini where they play an important role in controlling the release of neurotransmitters (Wang et al. 2001). When an action potential reaches the terminal of a neuron, voltage-dependent Ca^{2+} channels open and allow the influx of Ca^{2+}, that stimulate vesicle fusion and neurotransmitter release. The increase in intracellular Ca^{2+} also activates BK_{Ca} channels that repolarize the membrane potential with a big outward conductance of K^+. Thus BK_{Ca} channel works as a negative feedback for Ca^{2+} influx, limiting the release of neurotransmitters. In fact BK_{Ca} channels colocalize with Ca^{2+} channels in various neuronal cell types (Marrion and Tavalin 1998).

The first structural gene of BK_{Ca}-channel was derived from the slowpoke (‘*slo*’) gene of *Drosophila melanogaster* (Atkinson et al. 1991). Homologous of the *Drosophila* BK_{Ca} channel have been identified (named ‘*slo*’ cDNAs) in many species, including mouse and human (Tseng-Crank et al. 1994), and three *slo*-related genes were found (*slo1, slo2, slo3*).

3.2 Structure of BK_{Ca} channel

BK_{Ca} channels are homotetramers: each subunit consists of seven transmembrane segments and a large cytoplasmic C-terminus. Four α-subunits alone form a func-

Roberta Gualdani, *Using the Patch-Clamp technique to shed light on ion channels structure, function and pharmacology*, ISBN 978-88-6655-452-3 (print), ISBN 978-88-6655-453-0 (online)

tional channel (Shen 1994), while β-subunits play a modulatory role (Orio and Latorre 2005).

In Figure 3.1 is shown the proposed membrane topology of the BK_{Ca} α-subunit. This protein (~1200 amino acids) is arranged like a voltage-gated K^+ channel subunit, with the S4 helix that forms the channel's voltage-sensor, and a K^+-channel pore sequence. Contrary to K_v channel subunits, BK channel has an extra transmembrane segment at its N-terminus, termed S0 (Wallner et al. 1996), that is oriented toward the outside of the cell. BK channel contains also a large (~800 amino acid) C-terminal extension that comprises two Ca^{2+}-sensing regions termed RCK1 and RCK2 (Jiang et al. 2001, Schreiber and Salkoff 1997, Yuan et al. 2010, Yusifov et al. 2008, Wu et al. 2010).

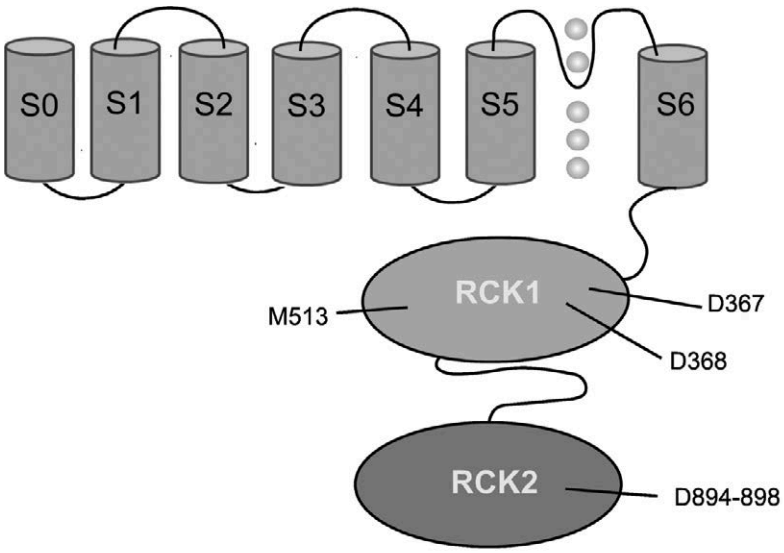

Figure 3.1 Membrane topology of the α-subunit of the BK_{Ca} channel. This subunit is composed of seven transmembrane domains, a K^+-selective pore and a large cytosolic C-terminal domain which comprises two Ca^{2+}-sensing modules termed RCK1 and RCK2 (Regulators of K^+ Conductance). The residues indicated are involved in the high-affinity Ca^{2+} sensitivity.

3.3 Ca^{2+} sensitivity of BK_{Ca} channel

It's known that Ca^{2+} sensitivity of BK_{Ca} channel is conferred by the large intracellular C-terminal region of the channel; however the regions of the BK_{Ca} channel involved in Ca^{2+} sensitivity are still under intense investigation.

Site-directed-mutagenesis experiments have shown that the Slo1 subunit appears to contain three types of Ca^{2+} binding sites (Xia et al. 2002, Zeng et al. 2005): one with low affinity (mM), that is disabled by mutations at positions E374 or E399 on RCK1 domain; two with higher affinity (μM), one that lies within the RCK1 do-

main and another that lies in a region of the channel known as the 'Ca^{2+} bowl' (D894-898).

The high-affinity RCK1 site can be disabled by mutations at positions M513, D362 or D367; similarly, neutralization of critical residues of Ca^{2+} bowl in RCK2 dramatically reduces Ca^{2+} sensitivity.

When mutations are made at all three sites together the channel's Ca^{2+} sensitivity is completely eliminated.

Recently the study of the Ca^{2+} sensing mechanism of the BK_{Ca} channel was greatly advanced by the publication of two crystal structures of the C-terminal domain of the channel (Yuan et al. 2010, Wu et al. 2010). Both structures indicated that each Slo1 subunit contains two structurally homologous domains -RCK1 and RCK2- that form a dimer-like structure, and four of these dimer-like structures form together a ring known as ' gating ring'.

Figure 3.2 Crystal structure of the BK_{Ca} channel's gating ring (PDB code 3NAF).

However, dispite these recent advances on the structure of the BK gating ring, the functional properties linked to its Ca^{2+} sensitivity have not yet been investigated and other mutagenesis and biochemical experiments are required.

The aim of this project was to identify some residues directly or indirectly involved in the coordination of Ca^{2+} ions in the RCK1 domain.

To this purpose, the structure-based multiple sequence alignment between the hSlo C terminus and several prokaryotic K^+ channel RCK domains is shown in Figure 3.3. The secondary structure assignment is based on the crystal structure of the MthK RCK domain (Protein Data Bank code 2AEF).

Bars and arrows show helices and extended strands, respectively; light grey highlighted residues are the semiconserved sequences. Residues in dark grey are critical for high-affinity Ca^{2+} sensitivity (D362/D367/M513 on RCK1 and D894–898 RCK2) and low-affinity Ca^{2+}/Mg^{2+}-binding site (E374/E399 and MthK D184/E210/E212, Yusifov et al. 2008).

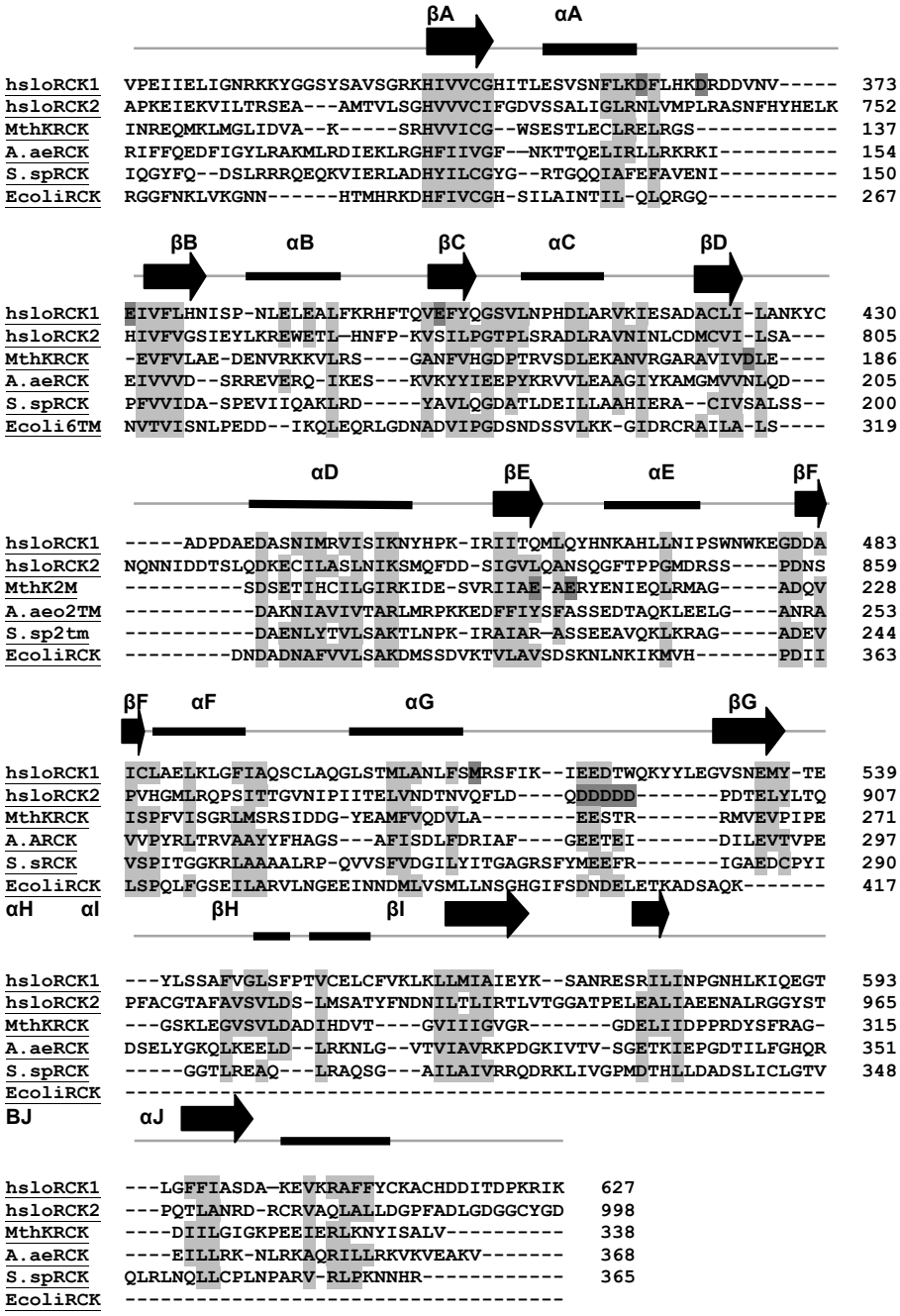

Figure 3.3 Structure-based multiple sequence alignment of the C terminus of the human BK_{Ca} channel and RCK domains of prokaryotic K^+-channels (Adapted from Yusifov et al. 2008).

3.4 Methods

Channel Expression in Oocytes

Oocytes were dissected from anesthetized *Xenopus leavis* (African clawed frogs) by surgical harvest of oocytes. Oocytes were immediately treated with collagenase (2mg/mL) for 1.5 hours, rinsed with a Ca^{2+}-free OR-2 solution (82.5 mM NaCl, 2.5 mM KCI, 1 mM $MgCl_2$, 5 mM Hepes-NaOH pH 7.6) and stored in SOS solution (96 mM NaCl, 2 mM KCI, 1.8 mM $CaCl_2$, 1 mM $MgCl_2$, 5 mM Hepes-NaOH pH 7.6, 100 units/ ml fresh penicillin, 100 μg/ml streptomycin, 50 μg/ml gentamycin).

The BK_{Ca}-subunit clones (wild type and mutants) were propagated in the *E.coli* strains XL1-blue. In vitro transcription was performed with the 'mMessage mMachine' kit (Ambion) with T3 RNA polymerase, using a NotI restriction enzyme for the linearization. All mutations were made with the Quick Change Site-directed mutagenesis and mutations were identified by sequencing around the point of the mutation. cRNAs encoding for the *hSlo* wild type and mutants were injected in *Xenopus laevis* oocytes (0.2 mg/ml), and K^+ currents were recorded by the patch-clamp technique (inside-out configuration) 2-3 days after injection.

Electrophysiology

Patch pipettes were pulled from glass capillary tubing (Warner G85150T-4) on a programmable Flaming/Brown type puller (Sutter P-97) and fire polished on a microforge (Narishige). Polished pipettes were approximately 2 μm in diameter and produced resistances ~2-3 MΩ. Patch pipettes were applied to the surface of a devitellinized oocytes to form electrical seals (>1 GΩ). Patches were excised in an inside-out configuration, exposing the cytoplasmic face membrane to a bath solution.

Data were acquired using an Axopatch 200B patch-clamp amplifier (Axon Instruments, Inc.). All experiments were performed at room temperature, 22–24°C. Solutions contain 115 mM KMES, 5 mM KCl, 10 mM Hepes, and 5 mM HEDTA. The free [Ca^{2+}] was measured using a Ca^{2+}electrode (World Precision Instruments). Conductance-voltage (G-V) relations were determined from the amplitude of the current measured to a fixed membrane voltage (0 mV) after voltage steps between -190 and +190 mV.

Each G-V relation was fitted by a Boltzmann function:

$$P_0 = \frac{G}{G_{MAX}} = \left[1 + \exp(-z_{eq} F(V - V_{1/2}) / RT)\right]^{-1} \qquad \textit{(Eq. 3.1)}$$

where P_o is the probability of channel opening, $V_{1/2}$ the voltage at which P_o is 0.5, z_{eq} is the equivalent gating charge associated with the closed to open transitions, and R, T and F have their usual meanings.

G-V relations were normalized to the peak of the fit.

3.5 Results

3D Homologing Modeling of RCK1 domain

The 3D homology model of RCK1 based on the structure of a bacterial RCK domain is shown in Figure 3.5; we observed that D362 and D367 (two residues important for Ca^{2+} sensitivity) map within the N-lobe, while M513 is part of the αG-βG loop. Moreover two positive charged residues, R514 and K518, are in proximity of D362/367, adjacent to M513. In particular distances between the Lysine518 N atom and the Glutamate362 and 367 carbonyl chains are, respectively, 16Å and 14 Å (Figure 3.4A), whereas between the Arginine514 N atom and the Glutamate362 and 367 carboxylate O atoms are 15Å and 21 Å (Figure 3.4B). Furthermore the αG-βG loop connecting the N and C lobes of RCK1 includes three consecutive negative residues: 520EED522 (Figure 3.4C), close to M513, that share significant homology with the high affinity Ca^{2+}-binding site ('Ca^{2+}-bowl' region) located in RCK2 domain.

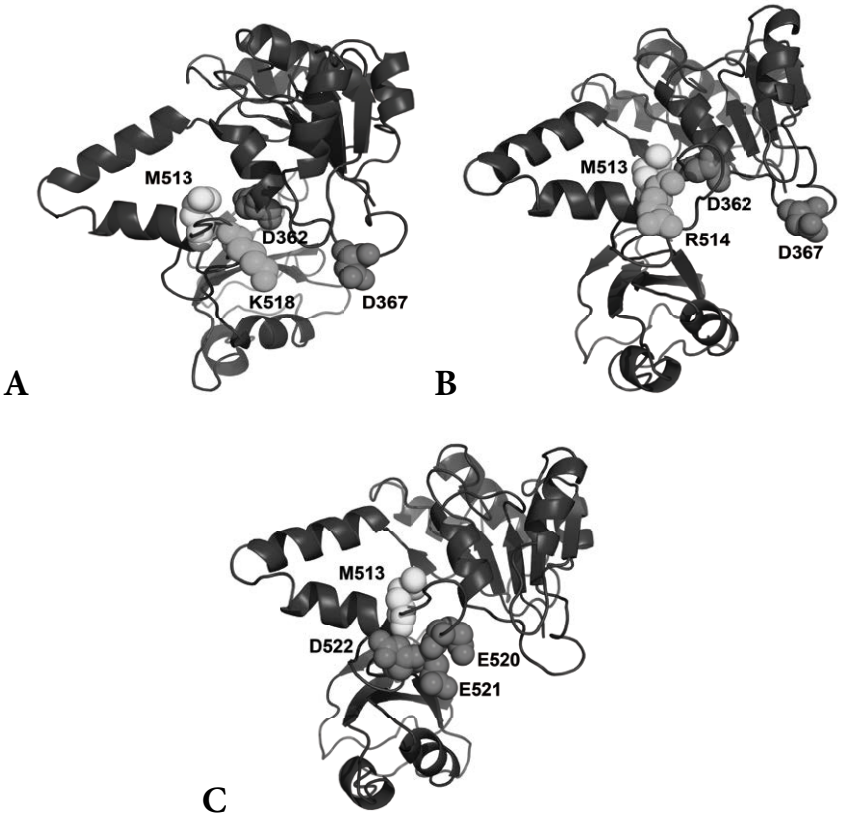

Figure 3.4 3D homology model of RCK1 based on the crystal stucture of MthK RCK (PDB 2AEF). Distances between K518 N atom and and D362/367 carbonyl chains are 16 Å and 14 Å respectively (A); distances between R514 N atom and D362/367 carboxylate atoms are 15 Å and 21 Å respectively (B).

Starting from these observations, we hypothesized that electrostatic interactions between K518 and R514 and D362/367 can be crucial for Ca^{2+}-binding, as well as the 520EED522 residues may play an important role in the Ca^{2+}-sensitivity of BK_{Ca} channels. To test this hypothesis we have mutated R514, K518 and 520EED522 amino acids and investigated their effects on the Ca^{2+}-dependent activation of channel through electrophysiological studies.

Effect of mutations of K518, R514 and EED520-522 residues on Ca^{2+} sensitivity of BK_{Ca} channel

The BK_{Ca} channel is both Ca^{2+} and voltage sensitive, and the combined effect of these stimuli is often displayed as a series of G-V curves determined at several Ca^{2+} concentrations. At each Ca^{2+} concentration the channel open probability (P_0) increases with membrane depolarization; as the Ca^{2+} concentration increases, less depolarized membrane potentials are required to activate the channels.
Using homology modeling we identified some residues that might contribute to the binding of Ca^{2+}: R514, K518, EED520-522. Using site-directed mutagenesis and electrophysiology we tested the relative contribution of the identified residues to a putative binding region for Ca^{2+}. In particular we mutated R514 and K518 residues to Ala and Glu individually; moreover we neutralize simultaneously EED520-522 residues to QQN (GlnGlnAsn) 520-522 mutant. Then we investigated their voltage and Ca^{2+} dependence of steady state inactivation.

To examine, in detail, the effects of Ca^{2+} and voltage on mutants activity we measured channel open probability (P_O) over a range of Ca^{2+} concentrations and membrane potentials. Figures 3.5-3.7 show macrocurrents (top) and P_O-voltage relationships (G/V curves, bottom) obtained at different Ca^{2+} concentrations, for BK_{Ca} channel wild-type and mutants. At each concentration, the G/V curve can be fitted by a single Boltzmann.

Figures 3.8-3.10 show the relationship between the 'Half maximal activation voltage' ($V_{1/2}$) of each mutant plotted against the Ca^{2+} concentration: as we can observe, $V_{1/2}$ shifted to more negative values as the calcium concentration increased.

Our results show that channels with mutations at positions K518 (Figure 3.8) and R514 (Figure 3.9), in the [Ca^{2+}] range between 0,01 and 10 μM, have a significant reduction of $V_{1/2}$ compared to wild-type. This means that the open probability of these mutants, at a given Ca^{2+} concentration, is higher than WT channels and thereby, because the *G–V* shift resulting from the mutation depends on [Ca^{2+}], also the Ca^{2+} sensitivity of these mutants is larger, compared to wild-type hSlo1 channel; on the contrary, the EED520-522QQN neutralization had little effect on Ca^{2+} dependence (Figure 3.10).

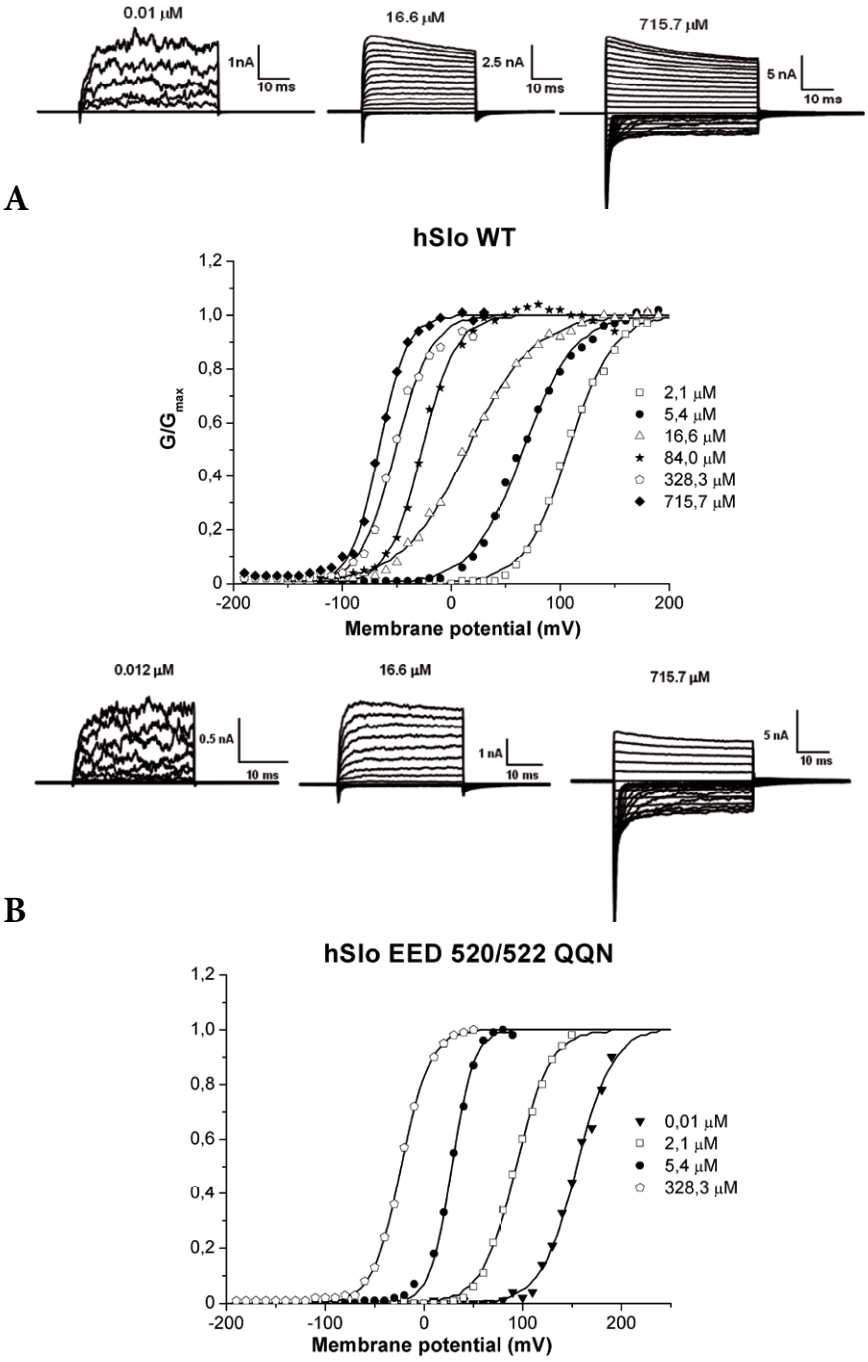

Figure 3.5 Macroscopic current traces (top) recorded with voltage step between -190 mV and +190 mV at different internal [Ca^{2+}]; G-V relationship (bottom) determined from patching expressing wild type BK_{Ca} channel (A) and EED520-522QQN mutant.

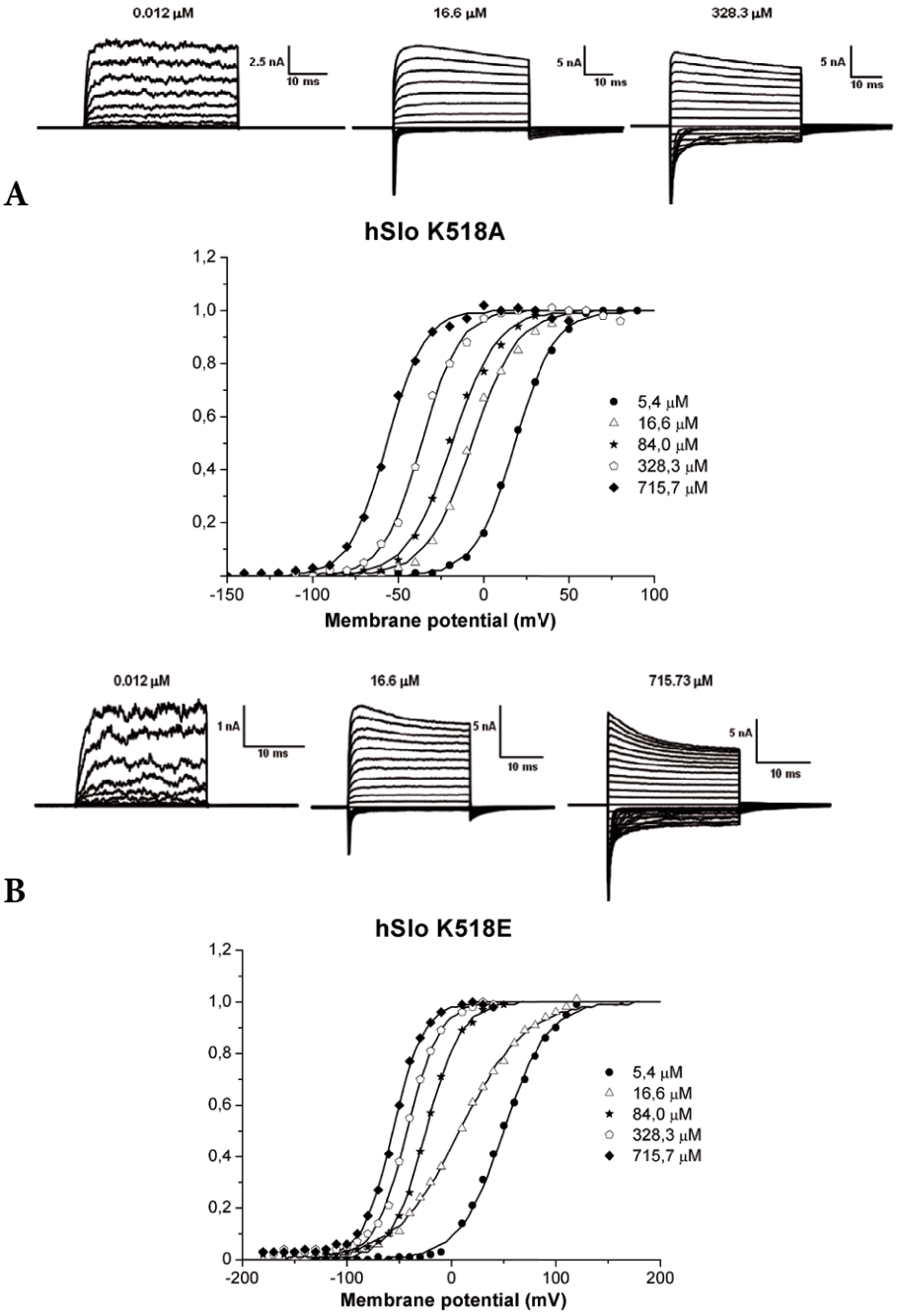

Figure 3.6 Macroscopic current traces (top) and G-V relationship (bottom) determined from patching expressing the BK_{Ca} channels K518A (A) and K518E (B) mutants. Each data point is the average of P_0 from two to five patches. At each Ca^{2+} concentration, the P_0-voltage relationship could be fitted by a single Boltzmann equation.

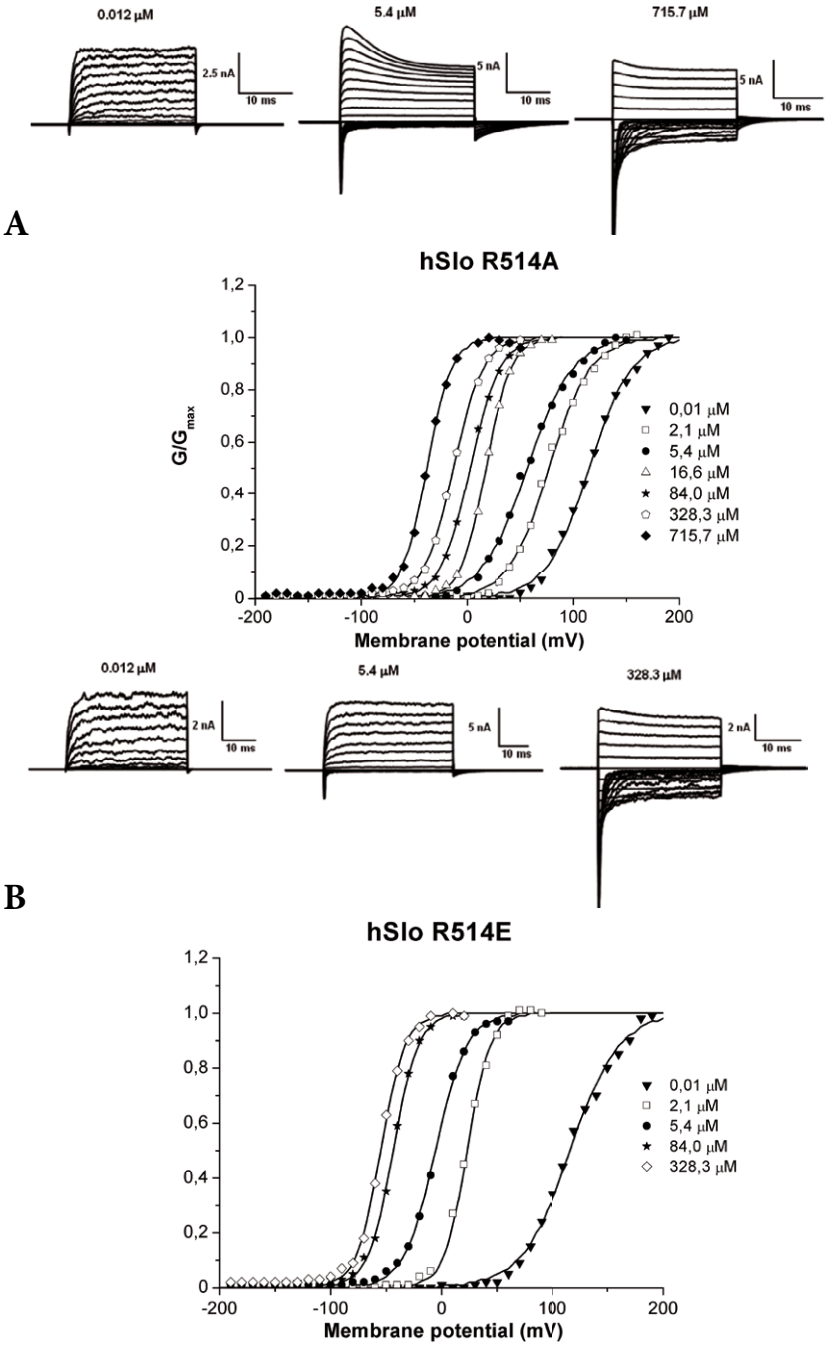

Figure 3.7 Macroscopic current traces (top) recorded with voltage step between -190 mV and +190 mV and G-V relationship (bottom) determined from patching expressing the BK_{Ca} channels R514A (A) and R514E (B) mutants, at different internal $[Ca^{2+}]$.

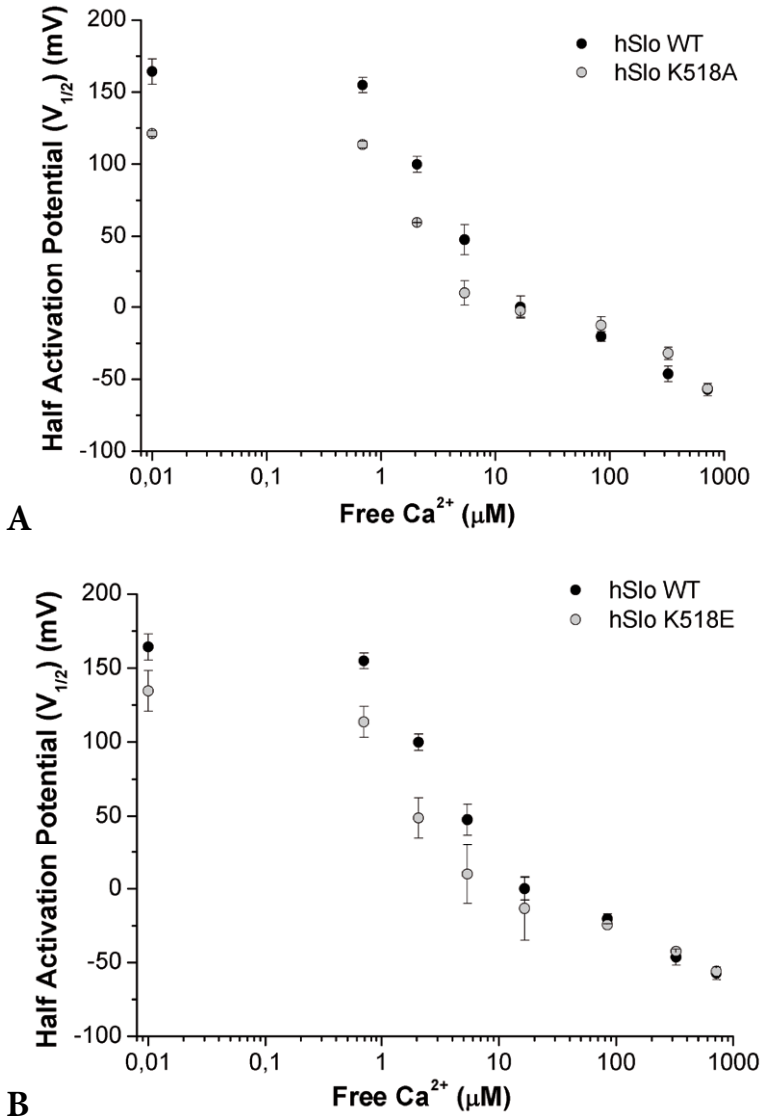

Figure 3.8 Half maximal activation voltage ($V_{1/2}$) plotted against [Ca^{2+}], for: wild type and K518A mutant (A); wild-type and K518E mutant (B). Each point is an average parameter values determined from experiments fitted individually with a Boltzmann function. Error bars represent standard error of the mean.

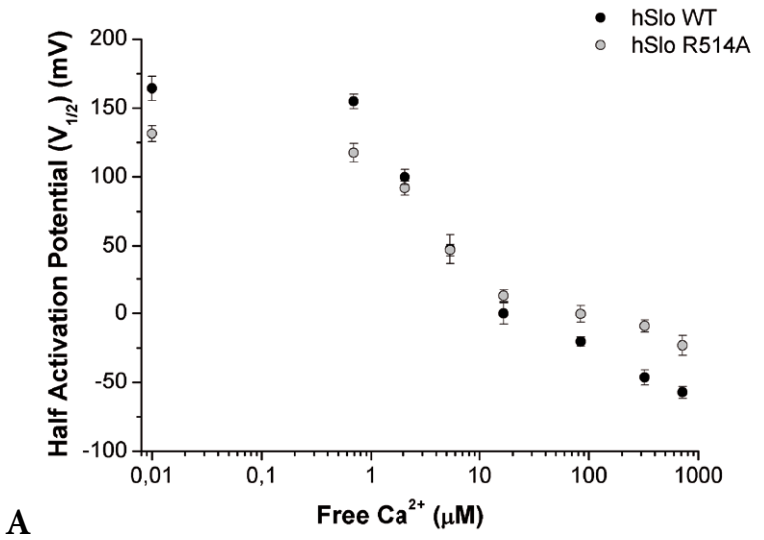

A

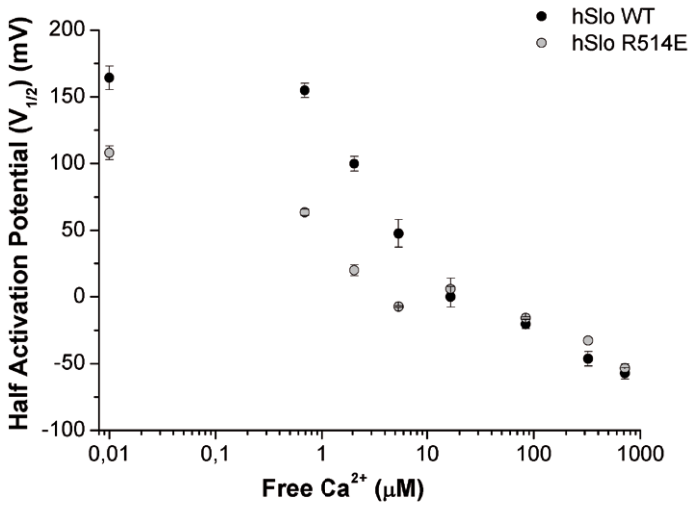

B

Figure 3.9 $V_{1/2}$ vs [Ca^{2+}] plot of WT and R514A mutant (A); WT and R514E mutant (B).

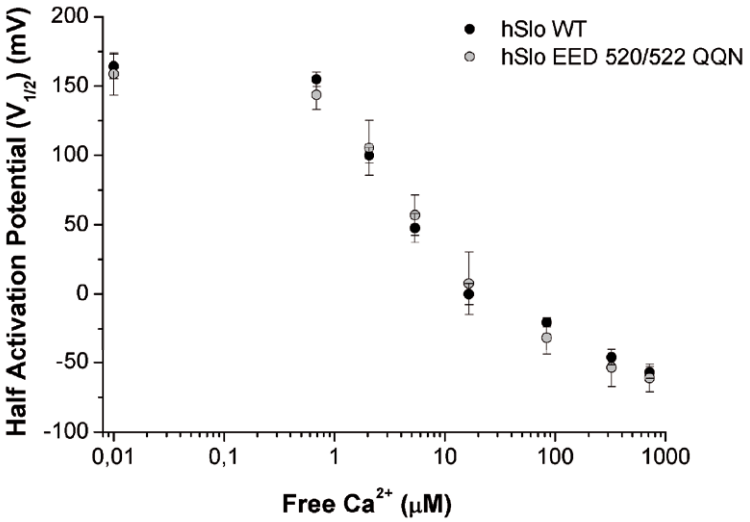

Figure 3.10 Half maximal activation voltage ($V_{1/2}$) plotted against [Ca^{2+}], for: wild type and EED520-522QQN mutant.

3.6 Discussion

The 3D homology model of RCK1 showed that two charged residues, R514 and K518 are in proximity of D362/367, adjacent to M513.
Our model was consistent with formation of electrostatic- like interactions (e.g. salt bridges) between these charged amino acids, because distances between the Lysine518 N atom and the Glutamate362 and 367 carbonyl chains are, respectively, 16Å and 14 Å (Figure 3.4A), whereas between the Arginine514 N atom and the Glutamate362 and 367 carboxylate O atoms distances are 15Å and 21 Å respectively (Figure 3.4B). Moreover, the αG-βG loop connecting the N and C lobes of RCK1 includes three consecutive negative residues: 520EED522 (Figure 3.4C), that share significant homology with the 'Ca^{2+} bowl' of RCK2 domain.

To test the role of these amino acids we have investigated the effect on Ca^{2+} sensitivity of charge neutralization/substitution at positions R514, K518 and EED520-2 on the Ca^{2+}-dependent activation of the human BK_{Ca} channel expressed in *Xenopus* oocytes using the patch clamp technique.

The Lys518 was mutated to Ala (K518A) and Asp (K518E); the Arg514 was mutated to Ala (R514A) and Asp (R514E); the three negative residues AspAspGlu520-2 were neutralized to GlnGlnAsn 520-2 residues (EED520-522QQN).

Figures 3.5-3.7 showed the G-V relationships determined from patching oocytes expressing different mutants; we observed that Ca^{2+} shifts the G/G_{max} curve towards the left along the voltage axis and data are well fitted by using a Boltzmann function. Figures 3.8-3.10 show the Half maximal activation voltage ($V_{1/2}$) of wild-type and each mutants plotted against Ca^{2+} concentration. Our data show that the EED520-

522QQN neutralization had little effect on Ca^{2+} dependence (Figure 3.8), in agreement with (Bao et al. 2002).

On the contrary, channels with mutations K518X (Figure 3.9) and R514X (Figure 3.10) displayed, at a given Ca^{2+} concentration, a significant reduction of $V_{1/2}$ compared to wild-type and therefore an apparent increase of Ca^{2+} sensitivity

More specifically, the apparent reduction of half activation potential ($V_{1/2}$) of these mutants was present in the [Ca^{2+}] range 0,01-10 μM and was more evident for negative mutations (Figures 3.9B and 3.10B) than uncharged mutations (Figures 3.9A and 3.10A).

This suggests that R514X and K518X mutations are involved in the high affinity Ca^{2+}-binding site, because at concentration >10 μM the ($V_{1/2}$) *vs* [Ca^{2+}]' plots show the same trend as the wild-type;

Moreover these data suggest that K518 and R514 have a relevant role in channel activation, because mutations of these residues set the RCK1 domain in a conformation similar to an open state of channel.

References

Atkinson N.S., Robertson G.A. and Ganetzky B. (1991) A.component of calcium-activated potassium channels encoded by the Drosophila slo locus. *Science* 253, 551-555.

Bao L., Rapin A.M., Holmstrand E.C., and Cox D.H, (2002) Elimination of the BK_{Ca} Channel's High-Affinity Ca^{2+} Sensitivity. *J. Gen. Physiol.* 120, 173-189.

Bao L., Kaldany C., Holmstrand E.C. and Cox D.H. (2004) Mapping the BK_{Ca} channel's 'Ca^{2+} bowl': side chains essential for Ca^{2+} sensing. *J. Gen. Physiol.* 123, 475-489.

Cui J., Yang H. and Lee U.S. (2009) Molecular mechanisms of BK channel activation. *Cell. Mol. Life Sci.* 66, 852 - 875.

Horrigan F.T., Aldrich R.W. (2002) Coupling between Voltage Sensor Activation, Ca^{2+} Binding and Channel Opening in Large Conductance (BK) Potassium Channels. *J. Gen. Physiol.* 120, 267-305.

Hou S., Xu R., Heinemann S.H. and Hoshi T. (2008) Reciprocal regulation of the Ca^{2+} and H^{+} sensitivity in the SLO1 BK channel conferred by the RCK1 domain. *Nat. Struct. Mol. Biol.* 15, 403-410.

Jiang Y, Pico A, Cadene M, Chait BT, MacKinnon R (2001) Structure of the RCK domain from the E. coli K^{+} channel and demonstration of its presence in the human BK channel. *Neuron* 29 (3), 593–601.

Latorre R. and Brauchi S. (2006) Large conductance Ca^{2+}-activated K^{+} (BK) channel: activation by Ca^{2+} and voltage. *Biol. Res.* 39, 385-401.

Marrion N.V. and Tavalin S.J. (1998) Selective activation of Ca^{2+}-activated K^{+} channels by co-localized Ca^{2+} channels in hippocampal neurons. *Nature* 395, 900-905.

Orio P. and Latorre R. (2005) Differential effects of beta 1 and beta 2 subunits on BK channel activity. *J. Gen. Physiol.* 125, 395-411.

Schreiber M. and Salkoff L. (1997) A novel calcium-sensing domain in the BK channel. *Biophys. J.* 73, 1355-1363.

Shen K.Z., Lagrutta A., Davies N.W., Standen N.B., Adelman J.P., North R.A. (1994) Tetraethylammonium block of Slowpoke calcium-activated potassium channels expressed in

Xenopus oocytes: Evidence for tetrameric channel formation. *Pflugers Arch.* 426, 440-445.

Tseng-Crank J., Foster C.D., Krause J.D., Mertz R., Godinot N., DiChiara T.J., Reinhart P.H. (1994) Cloning, expression, and distribution of functionally distinct Ca^{2+}-activated K^+ channel isoforms from human brain. *Neuron* 13, 1315–1330.

Wallner M, Meera P, Toro L (1996). Determinant for beta-subunit regulation in high-conductance voltage-activated and Ca^{2+}-sensitive K^+ channels: an additional transmembrane region at the N terminus". *PNAS* 93 (25), 14922–7.

Wang L. and Sigworth F. J. (2009) Structure of the BK potassium channel in a lipid membrane from electron cryomicroscopy. *Nature* 461, 292-295.

Wu Y., Yang Y., Ye S. and Jiang Y. (2010) Structure of the gating ring from the human large conductance Ca^{2+}-gated K^+ channel. *Nature* 466, 393–397.

Xia X.M., Zeng X. and Lingle C.J. (2002) Multiple regulatory sites in large-conductance calcium-activated potassium channels. *Nature* 418, 880-884.

Yuan P., Leonetti M.D., Pico A.R., Hsiung Y. and MacKinnon R. (2010) Structure of the human BK channel Ca^{2+}-activation apparatus at 3.0 A resolution. *Science* 329, 182-186.

Yusifov T., Savalli N., Gandhi C.S., Ottolia M. and Olcese R. (2008) The RCK2 domain of the human BK_{Ca} channel is a calcium sensor. *PNAS* 105, 376-381.

Zeng X.H., Xia X.M. and Lingle C.J. (2005) Divalent cation sensitivity of BK channel activation supports the existence of three distinct binding sites. *J. Gen. Physiol.* 125, 273-286.

Blockade of *h*ERG K^+ channel by two novel quinazoline-derivatives antimalarial drugs

4.1 Drugs, Arrhythmia, and the hERG K^+ channel

The rhythm of the heart is controlled by a balance of ions flowing in and out of the individual cardiac cells. The three most important types of proteins governing the activity of the heart are Na^+, Ca^{2+}, and K^+ channels. When they work in concert, the activity of these ion channels gives rise to the action potential (Klabunde 2005).
Any alteration in the flow of these ions during the heartbeat can lead to serious arrhythmia, possibly culminating in sudden cardiac death.

The human ether-a-go-go related gene (hERG) protein forms the ion channel responsible for the I_{Kr} voltage gated potassium ion current, together with some accessory proteins, e.g. MiRP1 (Abbott et al. 1999). The I_{Kr} current contributes to cardiac repolarisation (phase 3 of action potential) and genetic mutations or blockade of hERG K^+ channel lead patients to long QT sindrome, named also 'Torsades de Pointes' arrhythmia, which is characterized by twisting of the QRS complex around the isoelectric line of the ECG (Curran et al. 1995, Roden et al. 1996, Sanguinetti et al. 1997, Sanguinetti and Mitcheson 2005).

Only recently has been considered a major medical problem that commonly used medications can induce arrhythmia. In fact, this problem was recognized widely in the early 1990s during the Cardiac Arrhythmia Suppression Trial (CAST), which investigated class I of anti-arrhythmic agents that block Na^+ channels.

Now is believed that drug-induced QT prolongation can serve as an important biomarker for the development of cardiac arrhythmias; as a consequence, many drugs associated with QT prolongation have been removed from the market by regulatory authorities over the past decade (Roy et al. 1996, Zou et al. 1999).

It's interesting that all cases of drug-induced QT prolongation can now be explained by an interaction with hERG channel. This finding has launched a massive effort of the pharmaceutical companies to understand what molecular properties dictate drug/hERG interactions and how they can be eliminated.

Indeed, drugs with very different chemical structures have been shown to be strong blockers of hERG. This observation underlies the difficulty to understand the structure-activity relationship of hERG channel.

A number of factors make hERG K^+ channel the binding target of many structurally different compounds (Sanguinetti and Mitcheson 2005, Kongsamut et al. 2002, Kang et al. 2003):

Roberta Gualdani, *Using the Patch-Clamp technique to shed light on ion channels structure, function and pharmacology*,
ISBN 978-88-6655-452-3 (print), ISBN 978-88-6655-453-0 (online) © 2013 Firenze University Press

Thr623, Ser624 and Val625, located at the basis of the pore helix, and Gly648, Tyr652, and Phe656, located within the S6 domain, are sites of interaction with drugs (Mitcheson et al. 2000). In fact, mutation of these residues reduced the sensitivity of hERG to blockade by terfenadine, cisapride, and MK-499. Thes data suggest that the inhibition is due to the spatial positions of these residues.

The large size of the cavity of the channel (around 12 Å), in compare to other K_v channels, can accommodate a wide range of chemical products.

Considerable variations within the chemical structure of a drug can be tolerated without significant reduction of the inhibitory effect. For example, Phe656 or Tyr652 could interact by hydrophobic or π-stacking interactions with a chemical compound, but also the absence of both interactions could be well tolerated.

Antimalarial drugs represent a chemically diverse group of compounds. Although these drugs are associated with a higher risk for QT prolongation, the literature is poor regarding their respective effects on cardiac ion currents in relation to their chemical structure and no clear structure activity relationships related to a risk of I_{hERG} inhibition have yet been elucidated.

The aim of this project was to investigate the proarrhythmic activity of two novel antimalarial drugs (NF1563 and NF1546) by patch-clamp recording on *Xenopus laevis* oocytes expressing hERG K^+ channel.

NF 1563 and NF1546 are two quinazoline derivatives with high antiplasmodial activity measured *in vitro* against human red blood cells infected with either the D10 or the W2 strain of *P. falciparum*.

4.2 Methods

cRNA in vitro transcription

The hERG clone was propagated in the *E.coli* strains TOP10. *In vitro* transcription was performed with the "mMessage mMachine" kit (Ambion) with T7 RNA polymerase, using a EcoRI restriction enzyme recognition site for the linearization. After quantification of the yield of the transcription reaction using gel electrophoresis, cRNA was dissolved in RNAase free water for oocytes injection. To record macroscopic current, cRNA encoding for the channel was injected in *Xenopus laevis* oocytes, and K^+ currents were recorded with the patch-clamp technique (cell-attached configuration) 2-3 days after injection.

Oocyte Preparation and Injection

Oocytes were dissected from anesthetized *Xenopus leavis* (African clawed frogs) by surgical harvest of oocytes. Oocytes were treated with collagenase (2 mg/mL) for 1 hours, rinsed with a Ca^{2+}-free OR-2 solution (NaCl 82.5 mM, KCI 2.5 mM, $MgCl_2$ 1 mM, Hepes-NaOH 5 mM pH 7.6) and stored in SOS solution (NaCl 96 mM, KCl 2 mM, $CaCl_2$1.8 mM, $MgCl_2$ 1 mM, Hepes-NaOH 5 mM pH 7.6, fresh penicillin 100 units/ ml, streptomycin 100 µg/ml, gentamycin 50 µg/ml).

Electrophysiological Experiments

hERG macrocurrents were recorded by cell-attached patch-clamp recordings 2-3 days after injection. The pipette and the bath solutions had the following composition: KOH 98 mM, $MgSO_4$ 1 mM, $CaCl_2$ 1.8 mM, HEPES 5 mM, Na-pyruvate 2.5 mM (pH 7.5 with methanesulfonic acid) (Jiang 1999).
NF1546 and NF1563 were prepared as 10 mM stock solutions in water and stored at -20°C. On the day of experiments, aliquots of the stock solutions were diluted to the desired concentrations with the bath solution. Patch pipettes were pulled from glass capillary tubing (Warner G85150T-4) on a programmable Flaming/Brown type puller (Sutter P-87) and fire polished on a microforge using the resistive heat from a platinum wire. Polished pipettes produced resistances ranging 1.5-2 MΩW in series with recording equipment. Patch pipettes were applied to the surface of freshly devitellinized oocytes to form electrical seals (>1 GΩ), allowing a voltage-clamp on patches of plasma membrane. Data were acquired using a Multiclamp 700B patch-clamp amplifier and a Digidata 1440A acquisition system with pClamp 10 software (Molecular Devices). All experiments were performed at room temperature, 22–24°C. Data analysis was carried out using Clampfit 10.2 software (Axon Instruments) and OriginPro 8.1 (OriginLab Corporation, Northampton, MA).

4.3 Results

"Mimicking the intramolecular hydrogen bond: synthesis, biological evaluation, and molecular modeling of benzoxazines and quinazolines as potential antimalarial agents"
S. Gemma, C. Camodeca, M. Brindisi, [...], R. Gualdani, […], M.R. Moncelli, [...], G. Campiani, S. Butini. J. Med. Chem**.** 55 (2012) 10387-1040

References

Abbott G.W., Sesti F., Splawski I., Buck M.E., Lehmann M.H., Timothy K.W., Keating M.T., Goldstein S.A.N. (1999) MiRP1 forms IKr potassium shannels with HERG and is associated with cardiac arrhythmia. *Cell* 97, 175–187.

Curran M.E., Splawski I., Timothy K.W., Vincent G.M., Green E.D., Keating M.T., (1995) A molecular basis for cardiac arrhythmia: HERG mutations cause long QT syndrome. Cell 80, 795–804.

Jiang M., Dun W., Fan J.S. and Tseng G.N. (1999) Use-Dependent 'Agonist' Effect of Azimilide on the HERG Channel. *J. Pharmacol. Exp. Ther.* 291, 1324-1336.

Kang J., Chen X.L., Wang H., Rampe D. (2003) Interactions of the narcotic l-R-acetylmethadol with human cardiac K^+ channels. *Eur. J. Pharmacol.* 458, 25-29.

Klabunde, R.E. (2005) *Cardiovascular Physiology Concepts.* Lippincott Williams & Wilkins.

Kongsamut S., Kang J., Chen X.L.;, Roehr J., Rampe D. (2002) A comparison of the receptor binding and HERG channel affinities for a series of antipsychotic drugs. *Eur. J. Pharmacol.* 450, 37-41.

Mitcheson J. S., Chen J., Lin M., Culberson C., and Sanguinetti M. C (2000) A structural basis for drug-induced long QT syndrome. *PNAS* 97, 12329–12333.

Roden D.M., Lazzara R., Rosen M., Schwartz P.J., Towbin J., Vincent M.G., (1996) Multiple mechanisms in the long-QT syndrome: current knowledge, gaps and future directions. *Circulation* 94, 1996–2012.

Roy M.L., Dumaine R., Brown A.M. (1996) hERG, a primary human ventricular target of the nonsedating antihistamine terfenadine. *Circulation* 94, 817-823.

Sanguinetti M.C., Jiang C., Curran M.E., Keating M.T. (1995) A mechanistic link between an inherited and an acquired cardiac arrhythmia: HERG encodes the I_{kr} potassium channel. *Cell. Physiol. Biochem.* 81, 299–307.

Sanguinetti M.C. and Mitcheson J.S. (2005) Predicting drug-hERG channel interactions that cause acquired long QT syndrome. *Trends Pharmacol. Sci.* 26, 119-124.

Zhou Z., Vorperian V.R., Gong Q., Zhang S., January C.T. (1999) Block of hERG potassium channels by the antihistamine astemizole and its metabolites desmethylastemizole and norastemizole. *J. Cardiovasc. Electrophysiol.* 10, 836-843.

.

The antimigraine compound Parthenolide, contained in the Tanacetum Parthenium, activates and desensitizes the TRPA1 channel.

5.1 TRP channels

Transient receptor potential (*TRP*) ion channels are an important class of membrane proteins widely expressed in the mammalian central and peripheral nervous systems. They were first found in the fruit fly *Drosophila*; later, they were discovered in vertebrates where TRP channels act as polymodal sensors because they are activated by different stimuli (e.g. temperature, mechanical stretch, chemical compounds...) in both excitable and non-excitable cells (Clapham 2003, Moran et al. 2004, Montell 2005, Ramsey et al. 2006, Benton 2008).
Based on sequence homology, the mammalian TRP superfamily can be subdivided into seven subfamilies: TRPC ('Canonical'), TRPV ('Vanilloid'), TRPM ('Melastatin'), TRPA ('Ankyrin'), TRPP ('Polycystin'), TRPML ('Mucolipin'), TRPN ('No mechanoreceptor potentials') (Venkatachalam 2007).

Six of these channels (the 'vanilloid' TRPV1, TRPV2, TRPV3 and TRPV4; the TRPM8 and the TRPA1) are expressed by a subpopulation of peripheral sensory neurons, with C- (unmyelinated) or Aδ-(thinly myelinated) fibers, where they promote a rapid influx of cations, thereby causing neuronal excitation and generation of pain signalling (Tominaga et al. 1998).

The properties of TRP channels, even within the same subfamily, can vary a lot. They have different selectivity to monovalent and divalent cations; moreover they are activated by a number of stimuli, such as physical stimuli (temperature, voltage, mechanical stress), chemical ligands, intracellular ions and lipid components of the cellular membrane. Also a single TRP channel can integrate different signals, thus acting as a polymodal sensor.

For example the TRP channels TRPV1, TRPM8 and TRPA1 are implicated in termal and pain sensation (Clapham et al. 2005, McKemy 2005), but they can be activated also by pungent compounds and modulated by inflammatory factors.

In accordance with this big diversity, TRP channels are implicated in a multitude of processes, ranging from Ca^{2+} and Mg^{2+} homeostasis and regulation of the vascular tone to taste perception and temperature sensing.

The importance of TRP channels in human health and disease is illustrated by the growing number of channellopathies that are caused by mutations in TRP channel genes, e.g. hypomagnesemia with secondary hypocalcemia (mutations in TRPM6), autosomal dominant brachyolmia (mutations in TRPV4), autosomal dom-

Roberta Gualdani, *Using the Patch-Clamp technique to shed light on ion channels structure, function and pharmacology*, ISBN 978-88-6655-452-3 (print), ISBN 978-88-6655-453-0 (online)

inant focal segmental glomerulosclerosis (mutations in TRPC6). Furthermore, TRP channels are implicated in other pathophysiological conditions including neuropathic pain, headache, cancer, asthma (Nilius 2007).

As a consequence, TRP channels are becoming a novel promising therapeutic target and bigger effort is made to understand their molecular function, cellular regulation and involvement in pathophysiology.

5.2 TRPA1 channel and Pain

The transient receptor potential ankirin 1 (TRPA1) is a receptors belonging to the largest family of TRP ion channels, which exert pleiotropic functions in a variety of cells. TRPA1 localizes to primary sensory neurons of the trigeminal, vagal and dorsal root ganglia (DRG).

More specifically, TRPA1 co-localizes with the vanilloid TRPV1 channel (also known as the 'receptor' for capsaicin, the hot principle contained in hot peppers) in a subset of somatosensory neurons with non-myelinated or thinly myelinated fibers (C/ Aδ- fibers) and with nociceptive and pain producing functions. These neurons contain and release the proinflammatory neuropeptides substance P (SP) and calcitonin gene-related peptide (CGRP), which mediate painful responses and neurogenic inflammation and vasodilatation.

The most recent topology of TRPA1 channel contains six transmembrane domains (TM1-TM6) and a long cytoplasmic N-terminal domain that contains a multiple ankyrin repeat domain and an EF-hand domain (Figure 5.1).

Pharmacological and biophysical experiments revealed that TRPA1 is activated by a number of pungent and irritant reactive chemical compounds including allyl isothiocyanate (mustard oil), cinnamaldehyde (cinnamon oil), allicin (onions), carvacrol (oregano), polygodial (Tasmanian pepper) and formaldehyde (formalin); all of these molecules elicit a painful burning and a prickling sensation.

TRPA1 is also activated by α,β-unsaturated aldehydes enriched in photochemical smog, cigarette smoke (acrolein, methacrolein, methyl vinyl ketone) and is also susceptible to the oxidative stress which causes neuropathic pain and natural physical stimuli including both cold and mechanical force (McNamara et al. 2003, Jordt et al. 2004, Bautista et al. 2006, Bandell et al. 2004, Andersson et al. 2008, Andre et al. 2008, Bessac and Jordt 2008).

These compounds activate TRPA1 through a mechanism different from the other classical ligand and receptor interaction; in particular they are membrane permeable electrophiles that can form covalent adducts with thiols, primary amines, and to some extent with hydroxyl group (Smith and March 2001) via Michael addition reaction. Moreover TRPA1 cysteine modification with AITC and cinnamaldehyde is reversible while using N-Methylmaleimide (NMM) is irreversible (Macpherson et al. 2007, Hinman et al. 2006).

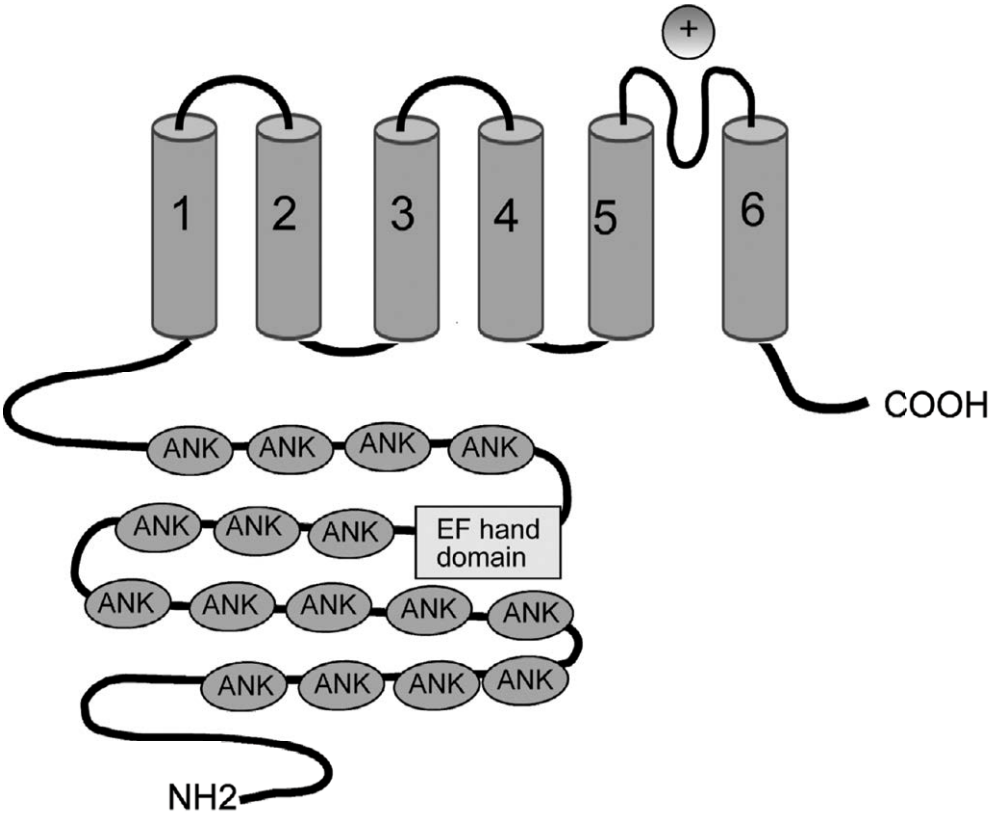

Figure 5.1 Four identical TRPA1 subunits combine to form a functional channel. As shown here, each subunit spans the plasma membrane six times (transmembrane domains TM1–TM6) and has a long cytoplasmic N-terminal domain. Ovals indicate ankyrin repeat domain, oblong indicates an EF-hand domain.

Because TRPA1 is considered as an attractive target involved in the generation and transmission of pain, novel covalent TRPA1 agonists have been discovered in the last 3 years and the biggest pharmaceutical companies (e.g. Merck Research Laboratories, Novartis Research Foundation, Hydra Biosciences, Eli Lilly) are already searching for effective TRPA1 modulators.

5.3 Parthenolide as a natural analgesic product

Parthenolide ((-)-Parthenolide) is a sesquiterpene lactone (Figure 5.2) that comes from the feverfew plant *(Tanacetum parthenium)* after which it is named.

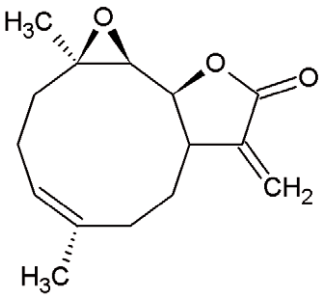

Figure 5.2 Structure of Parthenolide.

Parthenlide has been traditionally used in Europe to treat inflammatory diseases, such as fever, migraine, and arthritis, and as a digestive aid (Guzman et al. 2005, Tiuman et al. 2005, Miglietta et al. 2004, Feltenstein et al. 2004, Lopez-Franco et al. 2006, Yip et al. 2004).

The biological activity of PN is thought to be mediated through the α-methylene-γ-lactone moiety and the epoxide in its structure. These functional groups can react with nucleophiles, e.g. with cysteine thiol groups in a Michael addition reaction, to produce hemithioacetal products. However, the mechanism by which this occurs and the molecular targets of PN are unclear.

Since PN shares chemical similarity with established agonists of the TRPA1 channel, we speculated that Parthenolide could interact with TRPA1 channels.

In particular, for activation by noxious compounds, certain cysteine residues in the N-terminal intracellular domain of the TRPA1 channel are covalently bound and modified by highly reactive electrophilic compounds via Michael addition reaction and this also enables reactions of the cysteines with each other, which may modulate channel activation.

By electrophysiology we demonstrated that PN activates TRPA1 channel in a concentration-dependent manner and elicits desensitization and cross-desensitization in CHO cells expressing hTRPA1. Moreover, by site-direct mutagenesis, we showed that the triple mutant hTRPA1 (C619A C639A C663A) is less sensitive to PN and its sensitivity depends on the cellular redox state. We proposed that PN induces an irreversible modification of cysteine residues by formation of disulfide bonds, similarly to other TRPA1 agonists.

These data shed light on the mechanism of the analgesic activity of Parthenolide.

5.4 Methods

CHO cell culture

We used a tetracycline-regulated system for inducible expression of mouse TRPA1 in CHO (Chinese-Hamster Ovary) cells. To induce expression of TRPA1, 0.5 mg/ml

tetracycline was added to the culture medium, and cells were used 2-3 h after induction (Story et al. 2003).

Electrophysiology

For electrophysiological recordings in the whole-cell mode, CHO cells were maintaned in an extracellular recording solution containing: NaCl 150 mM, KCl 6 mM, $MgCl_2$ 1 mM, $CaCl_2$ 1.5 mM, HEPES 10 mM, glucose 10 mM, pH 7.4 (adjusted with NaOH). The pipette solution contained: NaCl 155 mM, $MgCl_2$ 1 mM, HEPES 10 mM, glucose 10 mM, pH 7.4 (adjusted with NaOH).

Mustard oil (allyl isothiocyanate), Parthenolide, Menthol, HC030031 were purchased from Sigma-Aldrich. For preparing stock solutions, they were dissolved in ethanol (Menthol) or DMSO (AITC/MO, Parthenolide, HC030031). Agonists were added from these stock solutions (100 mM) to the extracellular recording solution. The final ethanol/DMSO concentration in recording solution was <0.1%.

Patch-clamp electrodes were pulled from Sutter capillary glass (Novato, CA) on a Flaming/Brown type puller (Sutter P-87) and fire polished on a microforge (Narishige). Polished pipettes were approximately 2 μm in diameter and produced resistances ~3 MΩ. An Ag-AgCl wire was used as reference electrode.

Ionic currents were recorded using an Axopatch 200B amplifier (Molecular Devices, Inc., Sunnyvale, CA) and Digidata 1440 data acquisition board (Molecular Devices, Inc., Sunnydale, CA) with pCLAMP 10 software (Molecular Devices, Inc., Sunnyvale, CA). Data analysis was performed using Origin 6.1 (OriginLab Corporation, Northampton, MA).

Solutions were gravity fed through tubes connected to an 8-channel perfusion valve solution controller (Warner Instruments, Hamden, CT). Rapid bath solution exchange was achieved by placing the cell in a recording chamber (Warner Instruments, Hamden, CT) in front of a linear array of microperfusion pipes under computer control. All drugs used in our experiments were stored and handled following the manufacturer's instructions.

5.5 Results

"Parthenolide inhibits nociception and neurogenic vasodilatation in the trigeminovascular system by targeting TRPA1 channel"
Materazzi S, Benemei S, Fusi C, Gualdani R, De Siena G, Vastani N, Andersson DA, Trevisan G, Moncelli MR, Wei X, Dussor G, Pollastro F, Patacchini R, Appendino G, Geppetti P, Nassini R..
Pain 2013 Aug 8; doi: 10.1016/j.pain.2013.08.002.

References

Andersson D.A., Gentry C., Moss S., Bevan S. (2008) Transient receptor potential A1 is a sensory receptor for multiple products of oxidative stress. *J. Neuroscience* 28, 2485-2494.

Andre E., Campi B., Materazzi S., Trevisani M., Amadesi S., Massi D., Creminon C., Vaksman N., Nassini R., Civelli M., Baraldi P.G., Poole D.P.,Bunnett N.W., Geppetti P., Patacchini R. (2008) Cigarette smoke-induced neurogenic inflammation is mediated by alpha, beta-unsaturated aldehydes and the TRPA1 receptor in rodents. *Clin. Invest.* 118, 2574-2582.

Bandell M., Story G.M., Hwang S.W., Viswanath V., Eid S.R., Petrus M.J., Earley T.J., Patapoutian A. (2004) Noxious cold ion channel TRPA1 is activated by pungent compounds and bradykinin. *Neuron* 41, 849–857.

Bautista D.M., Jordt S.E., Nikai T., Tsuruda P.R., Read A.J., Poblete J., Yamoah E.N., Basbaum A.I., Julius D. (2006) TRPA1 mediates the inflammatory action of environmental irritants and pro-algesic agents. *Cell* 124. 1269-1282.

Benton R. (2008) Chemical sensing in Drosophila. *Curr. Opin. Neurobiol.* 4, 357-363.

Bessac B.F. and Jordt S.E. (2008) Breathtaking TRP Channels: TRPA1 and TRPV1 in Airway Chemosensation and Reflex Control. *Physiology (Bethesda)*, 23, 360-370.

Clapham D. (2003) TRP as cellular sensors. *Nature* 426, 517-24.

Feltenstein M.W., Schühly W., Warnick J.E., Fischer N.H., Sufka K.J. (2004) Anti-inflammatory and anti-hyperalgesic effects of sesquiterpene lactones from Magnolia and Bear's foot. *Pharmacology, biochemistry, and behavior* 79, 299–302.

Guzman M.L., Rossi R.M., Karnischky L., Li X., Peterson D.R., Howard D.S., Jordan C.T. (2005) The sesquiterpene lactone parthenolide induces apoptosis of human acute myelogenous leukemia stem and progenitor cells. *Blood* 105, 4163–4169.

Hinman A., Chuang H. H., Bautista D.M., Julius D. (2006) TRP channel activation by reversible covalent modification. *PNAS* 103, 19564–19568.

Jordt S.E., Bautista D.M., Chuang H., McKemy D., Zygmunt P.M., Högestätt E.D., Meng I.D., Julius D. (2004) Mustard oils and cannabinoids excite sensory nerve fibres through the TRP channel ANKTM1. *Nature* 427, 260-265.

López-Franco O., Hernández-Vargas P., Ortiz-Muñoz G., Sanjuán G., Suzuki Y., Ortega L., Blanco J., Egido J. (2006) Parthenolide modulates the NF-kappaB-mediated inflammatory responses in experimental atherosclerosis. *Arteriosclerosis, thrombosis, and vascular biology* 26, 1864–1870.

Macpherson L. J., Dubin A.E., Evans M.J., Marr F., Schultz P.G., Cravatt B.F. Patapoutian A. (2007) Noxious compounds activate TRPA1 ion channels through covalent modification of cysteines. *Nature* 445, 541–545

McKemy D. (2005) How cold is it? TRPM8 and TRPA1 in the molecular logic of cold sensation. *Molecular Pain* 1, 16.

McNamara C.R., Mandel-Brehm J., Bautista D.M., Siemens J., Deranian K.L., Zhao M. (2007) TRPA1 mediates formalin induced pain. *PNAS* 104, 13525-13530.

Miglietta A., Bozzo F., Gabriel L., Bocca C. (2004) Microtubule-interfering activity of parthenolide. *Chemico-biological interactions* 149, 165–173.

Montell C. (2005) Drosophila TRP channels. *Pflugers Arch.* 451, 19-28.

Moran M.M., Xu H., Clapham D.E. (2004). TRP ion channels in the nervous system. *Curr. Opin. Neurobiol.* 14, 362-369.

Nilius B. (2007) TRP channels in disease. *Biochim. Biophys. Acta* 1772, 805-812.

Ramsey S., Delling M., Clapham D. (2006) An introduction to TRP Channels. *Annu. Rev. Physiol.* 68, 619-647.

Smith M., March J. (2001). March's Advanced Organic Chemistry: Reactions, Mechanisms, and Structure. New York: Wiley.

Story G.M., Peier A.M., Reeve A.J., Eid S.R., Mosbacher J., Hricik T.R., Earley T.J., Hergarden A.C., Andersson D.A., Hwang S.W., McIntyre P., Bevan S. and Patapoutian A. (2003) ANKTM1, a TRP-like channel expressed in nociceptive neurons, is activated by cold temperatures. *Cell* 112, 819-829.

Tiuman T.S., Ueda-Nakamura T., Garcia Cortez D.A., Dias Filho B.P., Morgado-Díaz J.A., De Souza W., Nakamura C.V. (2005) Antileishmanial Activity of Parthenolide, a Sesquiterpene Lactone Isolated from Tanacetum parthenium. *Antimicrobial agents and chemotherapy* 49, 176–182.

Tominaga M., Caterina M.J., Malmberg A.B., Rosen T.A., Gilbert H., Skinne K., Raumann B.E., Basbau A.I., Julius D. (1998) The cloned capsaicin receptor integrates multiple pain producing stimuli. *Neuron* 21, 531-543.

Venkatachalam K., Montell C. (2007) TRP Channel. *Annu. Rev. Biochem.* 76, 387-417.

Yip K.H., Zheng M.H., Feng H.T., Steer J.H., Joyce D.A., Xu J. (2004) Sesquiterpene lactone parthenolide blocks lipopolysaccharide-induced osteolysis through the suppression of NF-kB activity. *J. Bone Min. Res.* 19, 1905–1916.

Acknowledgements

The research presented in this thesis has been carried out at the Department of Chemistry, University of Florence ('BioElectroLab') and at the Department of Anesthesiology, David Geffen School of Medicine, University of California Los Angeles (Prof. Riccardo Olcese's Lab).

I would like to gratefully acknowledge several people whose contribution has been essential for the accomplishment of this thesis.

First of all, I thank Prof. Maria Rosa Moncelli, whose supervision and energy have significantly contributed to the scientific success of this PhD.

Special thanks go to Prof. Riccardo Olcese, who has welcomed me as visiting researcher in his lab; I'm very grateful to him for introducing me to the world of electrophysiology and ion channels.

My sincere thanks go to Dr. Michela Ottolia (Cardiovascular Research Laboratory, UCLA) for her precious teaching about the Na^+-Ca^{2+} exchanger and the giant-patch technique.

Certainly, results of my work would not have been possible without the scientific commitment and friendship shared with Prof. Giorgio Rispoli (from the Department of Biology, University of Ferrara), 'BioElectroLab' members (Francesco, Gianluca, Serena, Alessio) and 'RO-lab' members (Taleh, Antonio, Azi, Roshni, Daniel).

Many thanks go to Jean Prenen and Prof. Thomas Voets (from Laboratory of Ion Channel Research, Katholieke Universiteit of Leuven) for teaching me how to measure TRPA1 currents and Prof. Pierangelo Geppetti for our useful discussions about TRP channels.

Roberta Gualdani, *Using the Patch-Clamp technique to shed light on ion channels structure, function and pharmacology*, ISBN 978-88-6655-452-3 (print), ISBN 978-88-6655-453-0 (online)

PREMIO TESI DI DOTTORATO

ANNO 2007

Bracardi M., *La Materia e lo Spirito. Mario Ridolfi nel paesaggio umbro*

Coppi E., *Purines as Transmitter Molecules. Electrophysiological Studies on Purinergic Signalling in Different Cell Systems*

Mannini M., *Molecular Magnetic Materials on Solid Surfaces*

Natali I., *The Ur-Portrait.* Stephen Hero *ed il processo di creazione artistica in* A Portrait of the Artist as a Young Man

Petretto L., *Imprenditore ed Università nello start-up di impresa. Ruoli e relazioni critiche*

ANNO 2008

Bemporad F., *Folding and Aggregation Studies in the Acylphosphatase-Like Family*

Buono A., *Esercito, istituzioni, territorio. Alloggiamenti militari e «case Herme» nello Stato di Milano (secoli XVI e XVII)*

Castenasi S., *La finanza di progetto tra interesse pubblico e interessi privati*

Colica G., *Use of Microorganisms in the Removal of Pollutants from the Wastewater*

Gabbiani C., *Proteins as Possible Targets for Antitumor Metal Complexes: Biophysical Studies of their Interactions*

ANNO 2009

Decorosi F., *Studio di ceppi batterici per il biorisanamento di suoli contaminati da Cr(VI)*

Di Carlo P., *I Kalasha del Hindu Kush: ricerche linguistiche e antropologiche*

Di Patti F., *Finite-Size Effects in Stochastic Models of Population Dynamics: Applications to Biomedicine and Biology*

Inzitari M., *Determinants of Mobility Disability in Older Adults: Evidence from Population-Based Epidemiologic Studies*

Macrì F., *Verso un nuovo diritto penale sessuale. Diritto vivente, diritto comparato e prospettive di riforma della disciplina dei reati sessuali in Italia*

Pace R., *Identità e diritti delle donne. Per una cittadinanza di genere nella formazione*

Vignolini S., *Sub-Wavelength Probing and Modification of Complex Photonic Structures*

ANNO 2010

Fedi M., *«Tuo lumine». L'accademia dei Risvegliati e lo spettacolo a Pistoia tra Sei e Settecento*

Fondi M., *Bioinformatics of genome evolution: from ancestral to modern metabolism. Phylogenomics and comparative genomics to understand microbial evolution*

Marino E., *An Integrated Nonlinear Wind-Waves Model for Offshore Wind Turbines*

Orsi V., *Crisi e Rigenerazione nella valle dell'Alto Khabur (Siria). La produzione ceramica nel passaggio dal Bronzo Antico al Bronzo Medio*

Polito C., *Molecular imaging in Parkinson's disease*

Romano R., *Smart Skin Envelope. Integrazione architettonica di tecnologie dinamiche e innovative per il risparmio energetico*

ANNO 2011

Acciaioli S., *Il* trompe-l'œil *letterario, ovvero il sorriso ironico nell'opera di Wilhelm Hauff*

Bernacchioni C., *Sfingolipidi bioattivi e loro ruolo nell'azione biologica di fattori di crescita e citochine*

Fabbri N., *Bragg spectroscopy of quantum gases: Exploring physics in one dimension*

Gordillo Hervás R., *La construcción religiosa de la Hélade imperial: El Panhelenion*

Mugelli C., *Indipendenza e professionalità del giudice in Cina*

Pollastri S., *Il ruolo di TAF12B e UVR3 nel ciclo circadiano dei vegetali*

Salizzoni E., *Paesaggi Protetti. Laboratori di sperimentazione per il paesaggio costiero euro-mediterraneo*

Evangelisti E., *Structural and functional aspects of membranes: the involvement of lipid rafts in Alzheimer's disease pathogenesis. The interplay between protein oligomers and plasma membrane physicochemical features in determining cytotoxicity*

Bondì D., *Filosofia e storiografia nel dibattito anglo-americano sulla svolta linguistica*

Petrucci F., Petri Candidi Decembrii *Epistolarum iuvenilium libri octo*. A cura di Federico Petrucci

Alberti M., *La 'scoperta' dei disoccupati. Alle origini dell'indagine statistica sulla disoccupazione nell'Italia liberale (1893-1915)*

Gualdani R., *Using the Patch-Clamp technique to shed light on ion channels structure, function and pharmacology*

Adessi A., *Hydrogen production using Purple Non-Sulfur Bacteria (PNSB) cultivated under natural or artificial light conditions with synthetic or fermentation derived substrates*

Ramalli A., *Development of novel ultrasound techniques for imaging and elastography. From simulation to real-time implementation*